Table 1 Laboratory tests on admission

Test	Result
Hb	10.5 g/dL
Ht	32.6%
RBC	$367 \times 10^4/\mu L$
PLT	$22.2 \times 10^4/\mu L$
WBC	3200/μL
Na	144 mEq/L
K	3.1 mEq/L
Cl	100 mEq/L
Ca	11.7 mg/dL
IP	3.4 mg/dL
BUN	19.3 mg/dL
Cr	0.7 mg/dL
TP	6.4 g/dL
Alb	3.3 g/dL
ALP	226 IU/L
AST	37 IU/L
ALT	35 IU/L
LDH	333 U/L
CK	25 IU/L
Glu	126 mg/dL
CRP	0.2 mg/dL

1 Alb, ...; ALP, ...; ALT, ...; AST, ...; BUN, ...; CK, ...; CRP, ...; LDH, ...; PLT, ...; RBC, ...; TP, ...; WBC, ...

Table 2 Results of thyroid function test

Test	Result (normal range)
FreeT4	6.69 ng/dL (0.73–1.53)
FreeT3	13.27 pg/mL (1.63–3.20)
Thyroid stimulating hormone (THS)	0.015 IU/mL (0.41–5.27)
TSH receptor antibody	51.2% (15<)
TSAb (thyroid stimulatory antibody)	540% (180<)
Antithyroid peroxydase antibody	43.8 U/mL (0.3<)
Serum thyroglobulin autoantibodies	0.3 < U/mL (0.3<)

On laboratory tests (Table 1), she showed blood hemoglobin of 10.5 g/dL, white blood cell counts of 3200/μL and serum calcium of 11.7 mg/dL (corrected calcium of 12.4 mg/dL). Other electrolytes as well as liver and kidney function were normal. Thyroid function tests (Table 2) revealed marked hyperthyroidism; free T4 of 6.69 (reference, 0.90–1.70) ng/dL, free T3 of 13.27 (2.3–4.3) pg/mL and thyroid stimulating hormone (TSH) of <0.015 (0.5–5.0) μIU/mL. Plasma levels of TSH receptor antibody, thyroid stimulating antibody and anti-TPO antibody were elevated, compatible with the findings in Graves' disease. Plasma intact PTH was 13 (10–65) pg/mL and PTH-related protein was not detected.

Table 3 Results of markers of bone metabolism

Marker	Result (normal range)
Osteocalcin	9.5 ng/mL (2.5–13)
Bone-specific alkaline phosphatase	24.2 U/L (9.6–35.4)
p-N-telopeptides	43.3 nMBCE/L (10.7–24.0)
Deoxypyridinoline/Cr	43.8 nmol/L/nMCr (2.8–7.6)
calcitonin	33 pg/mL
1–25(OH)VitD$_3$	6 pg/mL (20–60)

Figure 1 X-ray of lumbar vertebrae.

As shown in Table 3, markers of bone resorption such as deoxypyridinoline (DPD) and N-telopeptides of collagen cross-links (NTx) were elevated, whereas those of bone formation such as osteocalcin and bone-type alkaline phosphatase were not. Bone mineral density of lumbar vertebrae was –3.29 (T score), and that of femur was –3.72 (T score). Multiple compression fractures and remarkable reduction in bone mineral density were found on spinal lateral X-rays and dual energy X-ray absorptiometry, respectively (Fig. 1).

Initially, vitamin D toxicity was suspected as a cause of hypercalcemia; thus, alphacalcidol was ceased with fluid infusion to wash out calcium. However, the

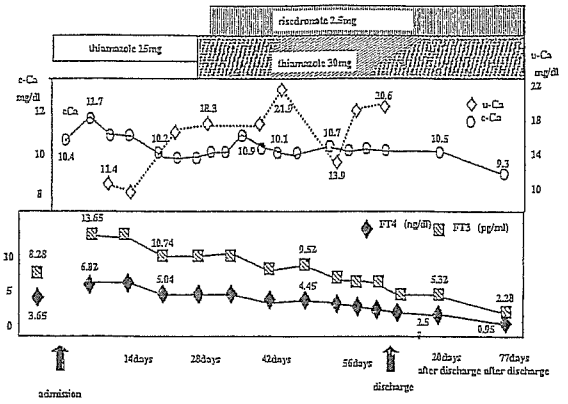

Figure 2 Clinical course of the patient. Thyroid stimulating hormone (TSH) was below the detection limit throughout the clinical course. c-Ca, collected serum calcium; u-Ca, urinary calcium; FT4, free thyroxine; FT3, free triiodothyronine.

hypercalcemia had not improved one week later. Laboratory and imaging tests were carried out to exclude hyperparathyroidism, humoral hypercalcemia of malignancy, osteolytic bone metastases and multiple myeloma. Finally, hypercalcemia was considered to be attributable to the exacerbation of hyperthyroidism with high bone turnover. Consequently, the dose of thiamazole was increased to 30 mg/day to normalize thyroid function. As shown in Figure 2, free T4 and free T3, as well as serum calcium were gradually decreased, and the patient was discharged on May 14 2004. In August 2004, her thyroid function returned to normal (free T4 of 0.95 ng/dL and free T3 of 2.28 pg/mL) with corrected serum calcium concentration of 9.2 mg/dL.

Discussion

Hypercalcemia associated with hyperthyroidism has been reported to occur more frequently in elderly patients than in younger patients; the incidence of hypercalcemia was 2.3% in hyperthyroid patients under 60 years of age and was 18.8% in those over 60 years of age.[2] The severity of hypercalcemia, however, is generally mild, ranging from the upper normal limit to the slightly elevated level,[3] and other complications should be suspected when serum calcium concentration is over 12 mg/dL.[7] Actually, case reports have shown that hyperparathyroidism is uncommonly associated with hypercalcemia in thyrotoxicosis.[8] Only several cases have been reported that hyperthyroidism was considered the only cause of hypercalcemia over 12.0 mg/dL.[9–11] In our case, laboratory tests and diagnostic imaging excluded hyperparathyroidism as well as malignant neoplasms. Furthermore, hypercalcemia was ameliorated in parallel with the improvement of hyperthyroidism, indicating that hypercalcemia resulted from hyperthyroidism.

Thyroid hormones play a critical role in bone development because hypothyroidism in childhood results in the impaired skeletal development.[12] In adults, thyroid hormones are important in the maintenance of bone mass. Thyroid hormone receptors are expressed in bone cells such as osteoblasts and osteoclasts.[12] In adult hyperthyroidism, there is increased bone remodelling, characterized by an increase in both bone resorption and formation, and an imbalance between bone resorption and formation, which results in bone loss and an increased risk for osteoporotic fracture.[12] In our case, however, the markers of bone resorption were elevated but those of bone formation were not. This pattern is consistent with the changes of bone metabolism in older osteoporotic patients,[13] but is different from that in hyperthyroidism as mentioned above. This might be due to the age-related decline in thyroid hormone signaling that leads to bone formation. However, no reports including animal experiments to support this hypothesis can be found so far. This should be investigated in the future.

Anti-thyroid drugs restore not only serum calcium levels[14] but also bone mineral density[15] in patients with thyrotoxic hypercalcemia. It has been also reported that a β blocker, propranolol,[16,17] and radioiodine therapy[10] may ameliorate thyrotoxic hypercalcemia. In our case, an increased dose of thiamazole normalized both thyroid function and serum calcium levels several months later, but bone mineral density was not increased. Longer time periods would be necessary to see the recovery of bone mass if possible.

References

1 Daniel T, Aran B. The skeletal system in thyrotoxicosis. In: Lewis EB, Robert DU, (eds). *Werner and Ingbar's the Thyroid*, 8th edn. Philadelphia, PA: A Wolters Kluwer Co., 2000; 659–666.
2 Szabo ZS, Ritzl F. Hypercalcemia in hyperthyroidism. Role of age and goiter type. *Klin Wochenschr* 1981; 59: 275–279.
3 Mosekilde L, Melsen F, Bagger JP *et al.* Bone changes in hyperthyroidism: interrelationships between bone morphometry, thyroid function and calcium-phosphorus metabolism. *Acta Endocrinol* 1977; 85: 515–525.
4 Dittmar M, Kahaly GJ. Immunoregulatory and susceptibility genes in thyroid and polyglandular autoimmunity. *Thyroid* 2005; 15: 239–250.
5 Cole DE, Vieth R, Trang HM *et al.* Association between total serum calcium and the A986S polymorphism of the calcium-sensing receptor gene. *Mol Genet Metab* 2001; 72: 168–174.
6 Akcay A, Ozdemir FN, Sezer S *et al.* Association of vitamin D receptor gene polymorphisms with hypercalcemia in peritoneal dialysis patients. *Perit Dial Int* 2005; 25: S52–S55.
7 Ryo M, Shigeru Y, Hyo ES *et al.* The parathyroid function in patients with hyperthyroidism. *Nippon Naibunpi Gakkai Zasshi* 1984; 60: 892–898.

8 Maxon HR, Apple DJ, Goldsmith RE. Hypercalcemia in thyrotoxicosis. *Surg Gynecol Obstet* 1987; 147: 694–696.
9 Inaba M, Hamada N, Itoh K *et al.* A case report on disequilibrium hypercalcemia in hyperthyroidism. Comparison of calcium metabolism with other patients with hyperthyroidism. *Endocrinol Jpn* 1982; 29: 389–393.
10 Akihan Z, Singh A. Hyperthyroidism manifested as hypercalcemia. *South Med J* 1996; 89: 997–998.
11 Reular JB, Wise RW, Thorpe JB. Anemia, renal insufficiency, and hypercalcemia in a man with hyperthyroidism. *South Med J* 1985; 78: 59–63.
12 Bassett JH, Williams GR. The molecular actions of thyroid hormone in bone. *Trends Endocrinol Metab* 2003; 14: 356–364.
13 Chan GK, Duque G. Age-related bone loss: old bone, new facts. *Gerontology* 2002; 48: 62–71.
14 Hedman I, Tisell LE. Life-threatening hypercalcemia in a case of thyrotoxicosis: clinical features and management. A case report. *Acta Chir Scand* 1985; 151: 487–489.
15 Diamond T, Julie V, Richard S, Ptrick B. Thyrotoxic bone disease in women: a potentially reversible disorder. *Ann Intern Med* 1994; 120: 8–11.
16 Shahshahani MN, Palmieri GM. Oral propranolol in hypercalcemia associated with apathetic thyrotoxicosis. *Am J Med Sci* 1978; 275: 199–202.
17 Mallette LE, Rubenfeld S, Silverman V. A controlled study of the effects of thyrotoxicosis and propranolol treatment on mineral metabolism and parathyroid hormon immunoreactivity. *Metabolism* 1985; 34: 999–1006.

〈原　著〉

超高齢者におけるクレアチニンクリアランス推定式の比較検討

平山　俊一[1)]　菊池　令子[2)]　井上慎一郎[2)]　塚原　大輔[2)]　末光　有美[2)]
小林　義雄[2)]　杉山　陽一[2)]　長谷川　浩[2)]　神崎　恒一[3)]　井上　剛輔[3)]
鳥羽　研二[2)]

要　約　目的：高齢患者は外来では24時間クレアチニンクリアランスの測定が困難であり，服用薬物数も多いため，クレアチニンクリアランス実測値をできるだけ正確に反映する推定式を利用することは臨床上重要である．対象：各種基礎疾患を有する85歳以上の超高齢者67名を含む入院高齢者143名（男性73名　女性70名　平均年齢82.9±8.6歳）．方法：4種のクレアチニンクリアランス推定式から得られた推定値と24時間クレアチニンクリアランスの実測値との相関を比較検討した．結果と結論：全体として今回の検討では超高齢者においてもCockcroft and Gaultの式による推定値が最もよい相関を示した．85歳以上の女性超高齢者において実測値と推定式の相関が低く，推定式の改定についても今後の検討課題と思われる．

Key words：超高齢者，クレアチニンクリアランス，推定式，Cockcroft and Gaultの式，安田の式

（日老医誌　2007；44：90-94）

緒　言

高齢社会の到来により，外来入院を問わず，高齢患者が増加の一途をたどっている．厚生労働省の推計によると，2004年度において85歳以上の超高齢者は273.4万人と報告されている[1)]．高齢者に腎排泄型薬剤を投与する際，適正な用量を設定するため腎機能を正確に評価する必要がある．腎機能を表す指標として，糸球体濾過量には一般的に内因性クレアチニンクリアランス（以下Ccrと略す）が使われている．クリアランス試験には24時間蓄尿が必要であるが，時間を要することや被験者に排尿，蓄尿という負担があり繁雑であることから外来で測定することは容易ではない．このため血清クレアチニン値（以下Scrと略す）からCcrを推定するいくつかの数式が提案されている．しかしこれらの数式は実際に投薬の必要な諸疾患を有する高齢者に当てはめる際，筋肉量の減少などのためScrによるCcr推定値と実測したCcrがかけ離れた値を取ることがある．外来の超高齢患者においても適切な薬物療法を行うためには腎機能を正確に評価する必要がある．このため種々の推定式による相関を調べどの推定式が最もよく超高齢者に適合するか検討を行った．

対象及び方法

杏林大学病院高齢医学科に2004年9月から2006年1月の間に入院した60歳以上の症例のうち，短期入院や，蓄尿不可能症例を除外し，尿道留置カテーテルを使用している患者や蓄尿が可能と判断された症例全例を対象にした．疾患や治療による除外は設けず，脳血管障害，感染症，経口摂取不良，利尿剤，補液などの様々な基礎疾患，治療を有する高齢者（平均年齢82.9±8.6歳（男性82.0±8.8歳　女性83.8±8.3歳））例を対象に行った．男女比及び84歳以下と85歳以上の症例数に偏りはなかった（表1）．対象高齢者全体の平均Scrは1.31±0.87mg/dlであった．身体測定，血液検査，尿検査などを測定し24時間蓄尿によるCcrを計算した．なお，Ccrは未補正のものを使用した．安田の式[2)]，Cockcroft and Gaultの式[3)]（以下C&G式と略す），折田の式[4)]，Walserの式[5)]の推定値を算出し，それぞれ推定値と実測値の相関を回帰分析，相関係数の差の検定により解析し比較検討した．さらに，層別解析として，84歳までの前期及び後期高齢者群76名と，85歳以上の超高齢者67名について男女別に層別解析を行った．

また実測値と推定式からの値との一致を箱ヒゲ図で求

1）S. Hirayama：東京薬科大学
2）R. Kikuchi, S. Inoue, D. Tsukahara, Y. Suemitsu, Y. Kobayashi, Y. Sugiyama, H. Hasegawa, K. Kouzaki, K. Toba：杏林大学病院高齢医学科
3）G. Inoue：都京村山老人ホーム診療所内科
受付日：2006.4.18，採用日：2006.7.12

表1　対象年齢分布

Age（歳）	n		
	男性	女性	全体
～84	42	34	76
85～	31	36	67
全体	73	70	143

め，値が外れ値となった症例については，患者の疾患や治療の背景，測定時の問題点について調査した．

本研究は，杏林大学高齢医学の入院に際して，CCr測定値を臨床研究に使用することを口頭で説明し同意を得て試行した．

(1) 安田の式

男性：Ccr（m*l*/min）＝（176－年齢）×体重（kg）÷（100×Scr（mg/100 m*l*））

女性：Ccr（m*l*/min）＝（158－年齢）×体重（kg）÷（100×Scr（mg/100 m*l*））

(2) Cockcroft and Gault の式

男性：Ccr（m*l*/min）＝（140－年齢）×体重（kg）÷（72×Scr（mg/100 m*l*））

女性：Ccr（m*l*/min）＝{(140－年齢）×体重（kg）÷（72×Scr（mg/100 m*l*））}×0.85

(3) 折田の式

男性：Ccr（m*l*/min）＝（－0.065×年齢－0.493×BMI＋33）÷（体重（kg）×Scr（mg/100 m*l*））×14.4

女性：Ccr（m*l*/min）＝（－0.052×年齢－0.202×BMI＋21）÷（体重（kg）×Scr（mg/100 m*l*））×14.4

(4) Walser の式

男性：Ccr（m*l*/min）＝7.57÷Scr（mM）－0.103×年齢＋0.096×体重（kg）－6.66

女性：Ccr（m*l*/min）＝6.06÷Scr（mM）－0.08×年齢＋0.08×体重（kg）－4.81

成　績

85歳未満の前期及び後期高齢者群において，安田，C&G，折田，Walser の推定値と24時間蓄尿による実測値の相関係数（r）は安田 r＝0.761，C&G　r＝0.761，折田 r＝0.693，Walser　r＝0.553 と安田の式，C&G 式で強い傾向があった．超高齢者群において，各々の推定式による推定値と実測値の相関係数は安田 r＝0.718，C&G r＝0.739，折田 r＝0.697，Walser r＝0.645 と，安田の式，C&G 式で相関が強い傾向があった（図1，図2）．超高齢者を男女に分け両群で各々の推定値と実測値の相関係数 r を比較したところ，男性で安田 r＝0.840，C&G r＝0.841，折田 r＝0.791，Walser　r＝0.736，女性で安田 r＝0.678，C&G　r＝0.690，折田 r＝0.667，Walser　r＝0.582 となり，男性に強い相関傾向があり，女性の相関係数は低かった（図3，図4）．また，超高齢者群において回帰係数を比較したところ，男性で安田＝0.796，C&G＝0.988，折田＝0.577，Walser＝0.375　女性で安田＝1.088，C&G＝1.262，折田＝0.776，Walser＝0.395 となった．

図5は超高齢者を男女で比較したものである．縦軸は実測値と推定値のずれの割合を示したもの（(実測値－推定値）×100/実測値）である．折田，Walser の式では，男女共に推定値が高く評価される傾向がある．

85歳以上の超高齢者での箱ひげ図における外れ値を検討し，実測値が高値となる6例の患者背景を調べた．輸液4例，利尿剤や Ca 拮抗薬など腎血流量を増加させる薬剤4例，腎不全2例，Scr 高値2例，心不全2例，CRP 高値2例であった．また，推定値が高値となる7例の患者背景を調べた．輸液5例，蓄尿不全または蓄尿少量4例，腎不全4例，癌3例，コントロール不良の糖尿病1例，胸水貯留，腹水貯留1例，肥満1例であった．

考　察

服用薬物数が多いほど薬剤有害作用の発現率は増加する傾向にある．また，加齢によってもその傾向は増加する[6]．その原因には加齢に伴う薬物動態学的・薬力学的な変化，多剤併用による相互作用，日常生活活動度（ADL）・認知機能の低下などが考えられるが，特に重大な原因として，腎機能の低下による相対的過量投与が挙げられる．Scr による腎機能の推定にはいくつか方法があるが高齢者，特に超高齢者になると筋肉量の低下により Scr が腎機能の低下と不相応な低値を示すことがしばしば見られる．Ccr 測定上の更なる問題点として正確な蓄尿の可否がある．加齢に伴う残尿，失禁の増加や患者自身による蓄尿もれなどにより，正確な24時間蓄尿が困難なことがある．1日尿量が少ないとき，Ccr 実測値と推定値のばらつきが大きいとの報告もある．今回は尿道留置カテーテルを使用している患者や蓄尿が可能と判断された患者の症例を対象とし，努めて正確な採尿を試みた．しかしながら，本来行うべきクリアランス法の実施には正確な蓄尿と安静を要し，判定に時間がかかるため実際の外来診療では実施困難なことが多い．従って Scr より Ccr を推定する種々の方法が提案されてきた．今回検討した安田の式，Cockcroft and Gault の式，折田の式，Walser の式は代表的な推定式であり Scr 値，性別，年齢，体重より Ccr を推定できる．C&G 式は欧米で最も広く用いられており欧米人によい相関を示して

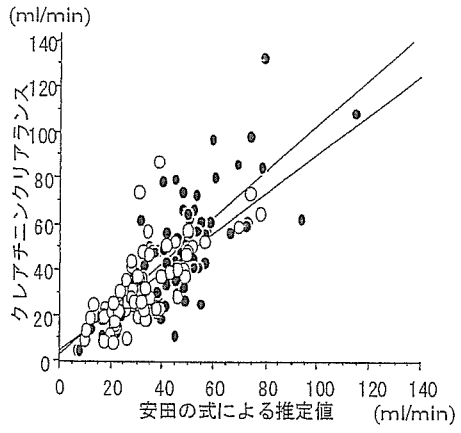

図1　安田の式　84歳以下と85歳以上の比較
○85歳以上；Y = 4.57 + 0.860X（r = 0.718）
●84歳以下；Y = 1.85 + 1.007X（r = 0.761）

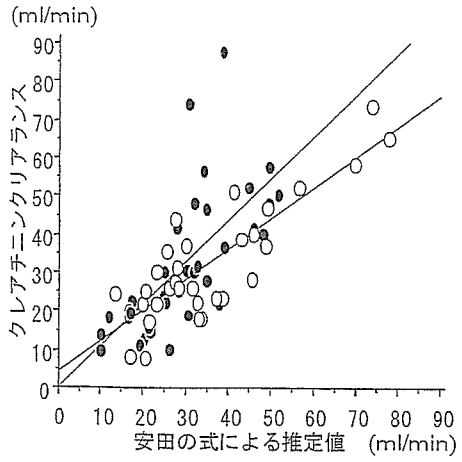

図3　安田の式　85歳以上の性差
○男性；回帰式 Y = 4.09 + 0.796X（r = 0.840）
●女性；回帰式 Y = 0.21 + 1.088X（r = 0.678）

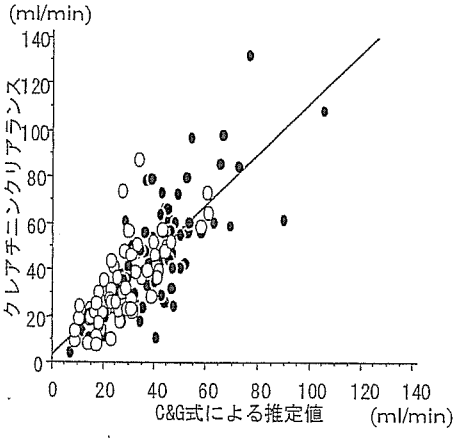

図2　C&G式　84歳以下と85歳以上の比較
○85歳以上；Y = 3.20 + 1.078X（r = 0.739）
●84歳以下；Y = 3.33 + 1.082X（r = 0.761）

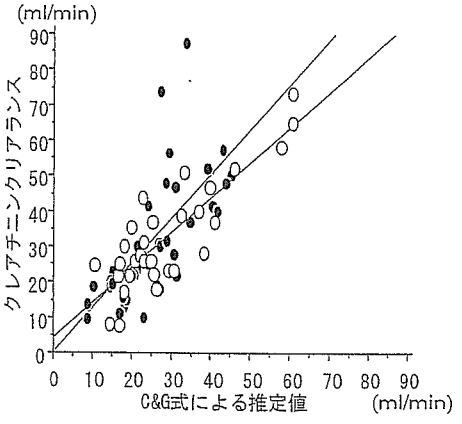

図4　C&G式　85歳以上の性差
○男性；回帰式 Y = 4.07 + 0.988X（r = 0.841）
●女性；回帰式 Y = − 0.09 + 1.262X（r = 0.690）

いる．今回の検討でも超高齢者における相関が0.739と最もよい相関を示した．この原因として日本人の体格が欧米化してきたことやC&G式作成時の対象年齢が18〜92歳と超高齢者も含まれていること，作成時の対象症例数が多いことが考えられる．C&Gの式に対して他の3式はいずれもその後に発表されたもので，安田の式は1.4mg/dl以下の血清クレアチニン値を示す高齢者に限定して式を求めたもので，腎不全患者は含めずに高齢者の腎機能を推定しようとしたものである[2]．一方，Walserの式は血清クレアチニン値を2.0mg/dl以上におき，腎不全患者のみを対象としている[5]．堀尾らの式は腎疾患患者を対象として，推定式にBMIの項を加えて肥満の特徴加味して作成された[4]．したがって，今回の対象のように腎機能が広範囲に亘る場合，C-Gの式以外では，いずれもずれが出てしまう結果となったのは，式の作成経緯による要素も大きいと考えられる．

今回，臨床の現場では安定した時期より外来や急性期での腎機能評価を必要とするため，疾患による除外は設けず，脳血管障害，感染症，経口摂取不良，利尿剤，補液などの様々な基礎疾患，治療を有する高齢者を対象に行った．推定式と実測値の乖離に関して，実測値が大きい場合は，輸液や降圧剤など腎血流量を増加させる治療が関与していた場合が多かった．この場合は臨床的には大きな実害は考えられない．一方，実測値が推定式より小さい場合は，相対的な薬物の過量投与など安全管理上

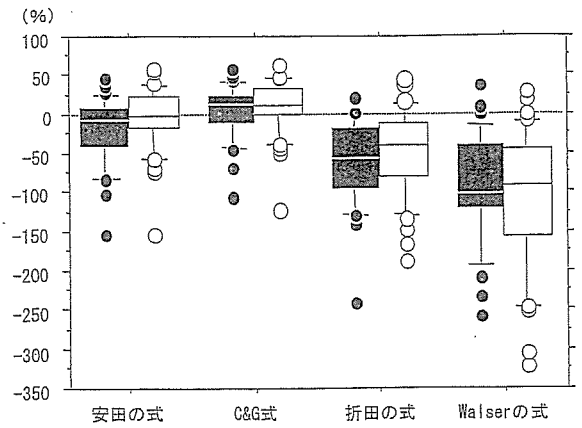

図5　超高齢者男女別において各推定式による推定値と実測値とのずれを箱ひげ図で％表示したもの
縦軸（実測値－推定値）×100/実測値
●男性
○女性

も問題となる．今回の検討では，腎不全，癌，乏尿，コントロール不良の糖尿病，胸水，腹水など複数の病態が重なる重症例で，有効循環血液量も日々変動しうる症例であった．このような症例に救急外来で遭遇した場合，血清クレアチニンから推定されるCcrの精度が低い可能性があることを銘記すべきであろう．Scrについては6.9までの高値も含まれているが，高値を除いた検討を行っても相関に大きな変化は見られなかった．全式において84歳までの前期及び後期高齢者群と85歳以上の超高齢者群に分け，相関を比較したところ，超高齢者群での相関が低い傾向にあり，超高齢者群での合併疾患の増加の影響が示唆される．これらを考慮しても，4種の推定式を比べると相関係数が最も高いC&G式が本邦超高齢者におけるCcr推定式として最適と考えられた．

超高齢者群を男女にわけC&Gの相関係数を比較したところ，男性0.841女性0.690と男性の相関が高い傾向にあった．また，回帰係数を比較したところ男性ではC&G式，女性では安田の式が1に近い値を示した．85歳以上の男性に安田の式を用いると過大評価する可能性があり，85歳以上の女性にC&G式を用いると過小評価する可能性がある．

一方，前期及び後期高齢者群の回帰係数を比較したところ男女ともに安田の式が1に近い値を示した．超高齢者の筋肉量について本邦での正確なデータは少ないが，中島らによれば70歳以降男性では上腕筋周囲，上腕筋面積が急速に減少するが女性ではほとんど変わらない[7]ことから女性の筋肉減少が時代とともに変化し，推定式の再構築が迫られている可能性があり，今後の検討課題と思われた．

本研究の限界として，膀胱留置カテーテルの適応がない蓄尿不可能症例を除外していることがあげられる．具体的には尿失禁症例や，認知症などが含まれるが，これらの症例に対してカテーテル留置を行ってクレアチニンクリアランスを測定し，高齢者全体に対するの推定式の良否を判断する研究は今後の課題であろう．

結　語

超高齢者において，正常値から腎不全を含む範囲の腎機能の判定に，24時間クレアチニンクリアランスの実測値と，すでに発表されている4つの式から求めた推定値とを比較して，超高齢者での推定式の有用性を検討した．4つの推定式のうち，C-Gの式はこの研究の目的にもっとも合致していた．一方，安田の式（高齢者，Scr: 1.4mg/dl以下），Wの式（Scr　2.0mg/dl以上）はいずれもその適用の目的の範囲で，また堀尾の式は腎疾患群内で有用と思われた．

全体として，臨床的に使用するうえでC&G式が最も優れているが，超高齢者への適用に当たっては，10%程度，推定値が低く求まるので，補正が望ましい．

今後超高齢者については，体格，サルコペニアの時代的変遷を考慮して改訂していく必要がある．

謝辞：本研究の一部は，長寿科学総合研究「縦断研究を基礎にした介護予防ガイドライン策定研究（H16痴呆骨折013；班長鳥羽研二），長寿医療研究事業「高齢者の安全な薬物療法ガイドライン策定研究(班長鳥羽研二）によった．

文　献

1) 厚生労働省ホームページ　平成17年度厚生統計要覧　総人口・日本人人口．性×年齢階級別．
2) 安田兵衛：腎機能の年齢的変化に関する研究．医学と生物学　1980; 101: 83-86.
3) Cockcroft DW, Gault MH: Prediction of Creatinine Clearance from Serum Creatinine. Nephron 1976; 16: 31-41.
4) Masaru Horio, Yoshimasa Orita, Shiro Manabe, Mitsuhiko Sakata, Megumu Fukunaga: Formula and Nomogram for Prediction Creatinine Clearance from Serum Creatinine Concentration. Clinical and Experimental Nephrology (1324-1751)　1997; 110-114.
5) Walser M, Drew HH, Guldan JL: Prediction of glomerular filtration rate from serum creatinine concentration in advanced chronic renal failure. Kidney International 1993; 44: 1145-1148.
6) 鳥羽研二，秋下雅弘，水野有三，江頭正人，金　承範，阿古潤哉ほか：薬剤起因性疾患．日老医誌　1999; 36: 181-185.
7) 中島久美子，秦　葭哉：身体組成としての筋肉量のアセスメント．日老医誌　2004; 42: 881-886.

Creatinine clearance estimation in the extremely elderly subjects

Shunichi Hirayama[1], Reiko Kikuchi[2], Shinichiro Inoue[2], Daisuke Tsukahara[2], Yumi Suemitsu[2], Yoshio Kobayashi[2], Yoichi Sugiyama[2], Hiroshi Hasegawa[2], Koichi Kouzaki[2], Gosuké Inoue[3] and Kenji Toba[2]

Abstract

Background: It has been reported that elderly outpatients take at least 6 different kinds of medication.

Purpose: To know which formula will best predict creatinine clearance, because 24-hour urine collection is difficult for elderly outpatients.

Patients and Methods: We compared four types of formulae (Cockcroft & Gault, Yasuda, Orita, Walser) to estimate creatinine clearance using serum creatinine of 143 elderly inpatients (73 men, 70 women, mean age 82.9±8.6 years old) including 67 extremely elderly people with various underlying diseases.

Result: The formula of Cockcroft and Gault showed the best correlation with creatinine clearance in the extremely elderly subjects ($r=0.74$) as well as in people under 85 years ($r=0.76$). However, the estimated values of the extremely elderly women were lower than actual creatinine clearance.

Conclusion: The formula of Cockcroft and Gault is the best predictive equation of creatinine clearance, except in the extremely elderly women.

Key words: *Extremely elderly, Creatinine clearance, Predicting formula, Cockcroft & Gault's formula, Yasuda's formula*
(Nippon Ronen Igakkai Zasshi 2007; 44: 90–94)

1) Tokyo University of Pharmacy and Life Science
2) Department of Geriatric Medicine, Kyorin University, School of Medicine
3) Department of Internal Medicine, Higashimurayama Nursing Home

Am J Physiol Cell Physiol 290: C208–C221, 2006.
First published August 31, 2005; doi:10.1152/ajpcell.00075.2005.

Role of calreticulin in the sensitivity of myocardiac H9c2 cells to oxidative stress caused by hydrogen peroxide

Yoshito Ihara,[1,2] Yoshishige Urata,[1] Shinji Goto,[1] and Takahito Kondo[1]

[1]*Department of Biochemistry and Molecular Biology in Disease, Atomic Bomb Disease Institute, Nagasaki University Graduate School of Biomedical Sciences, Nagasaki; and* [2]*Core Research for Evolutional Science and Technology, Japan Science & Technology Agency, Kawaguchi, Japan*

Submitted 22 February 2005; accepted in final form 29 August 2005

Ihara, Yoshito, Yoshishige Urata, Shinji Goto, and Takahito Kondo. Role of calreticulin in the sensitivity of myocardiac H9c2 cells to oxidative stress caused by hydrogen peroxide. *Am J Physiol Cell Physiol* 290: C208–C221, 2006. First published August 31, 2005; doi:10.1152/ajpcell.00075.2005.—Calreticulin (CRT), a Ca^{2+}-binding molecular chaperone in the endoplasmic reticulum, plays a vital role in cardiac physiology and pathology. Oxidative stress is a main cause of myocardiac apoptosis in the ischemic heart, but the function of CRT under oxidative stress is not fully understood. In the present study, the effect of overexpression of CRT on susceptibility to apoptosis under oxidative stress was examined using myocardiac H9c2 cells transfected with the *CRT* gene. Under oxidative stress due to H_2O_2, the CRT-overexpressing cells were highly susceptible to apoptosis compared with controls. In the overexpressing cells, the levels of cytoplasmic free Ca^{2+} ($[Ca^{2+}]_i$) were significantly increased by H_2O_2, whereas in controls, only a slight increase was observed. The H_2O_2-induced apoptosis was enhanced by the increase in $[Ca^{2+}]_i$ caused by thapsigargin in control cells but was suppressed by BAPTA-AM, a cell-permeable Ca^{2+} chelator in the CRT-overexpressing cells, indicating the importance of the level of $[Ca^{2+}]_i$ in the sensitivity to H_2O_2-induced apoptosis. Suppression of CRT by the introduction of the antisense cDNA of *CRT* enhanced cytoprotection against oxidative stress compared with controls. Furthermore, we found that the levels of activity of calpain and caspase-12 were elevated through the regulation of $[Ca^{2+}]_i$ in the CRT-overexpressing cells treated with H_2O_2 compared with controls. Thus we conclude that the level of CRT regulates the sensitivity to apoptosis under oxidative stress due to H_2O_2 through a change in Ca^{2+} homeostasis and the regulation of the Ca^{2+}-calpain-caspase-12 pathway in myocardiac cells.

apoptosis; calcium; endoplasmic reticulum

CALRETICULIN (CRT) is a Ca^{2+}-binding molecular chaperone expressed in the endoplasmic reticulum (ER) of a wide variety of eukaryotic cells (35). CRT is involved in many biological processes, including the regulation of Ca^{2+} homeostasis and intracellular signaling, glycoprotein folding, cell adhesion, gene expression, and nuclear transport (17, 23, 35).

CRT is well expressed in the embryonic rat heart, but its expression is suppressed after birth (21). It has been shown that CRT is essential for cardiac development in mice (33, 45). *CRT*-deficient embryonic cells showed an impaired nuclear import of nuclear factor of activated T-cell type 3 (NF-AT3), a transcription factor, indicating that CRT functions in cardiac development as a component of the Ca^{2+}/calcineurin/NF-AT/GATA-4 transcription pathway (33). On the other hand, *CRT*-transgenic mice experience complete heart block and sudden death (42). The CRT-dependent cardiac block involves an impairment of both the L-type Ca^{2+} channel and gap junction connexins 40 and 43 (Cx40 and Cx43, respectively). Also observed was a decrease in phosphorylated Cx43 in the *CRT*-transgenic heart, suggesting that the functions of protein kinases are altered via the regulation of Ca^{2+} homeostasis. CRT is also overexpressed in rat cardiomyocytes under pressure overload cardiac hypertrophy, implying some dysfunction of cardiomyocytes related to the overexpression (51). Furthermore, in cultured myocardiac H9c2 cells, overexpression of CRT after gene transfection promoted apoptosis during cardiac differentiation (24). In that study, the expression of protein phosphatase 2A (PP2A), a Ser/Thr protein phosphatase, was involved in altering the regulation of Akt signaling in H9c2 cells overexpressing CRT via an increase in the cytoplasmic free Ca^{2+} concentration ($[Ca^{2+}]_i$). Recently, we also reported that Akt signaling is important for cytoprotection against oxidative stress (39) and that a long-term change in $[Ca^{2+}]_i$ regulates *PP2Ac-α* gene transcription via the cAMP response element, resulting in a change in the activation status of Akt and leading to altered susceptibility to apoptosis (56). These studies suggest that CRT plays a vital role in myocardiac development and function, although the mechanism of this phenomenon has not been clarified fully.

An increasing body of evidence suggests that apoptosis plays an important role in cardiac development and disease (9, 12). Apoptosis occurs during reperfusion after ischemia in a variety of organs, including the heart (4). Oxidative stress with reactive oxygen species generated during ischemia-reperfusion injury is implied in the mechanism of cardiac damage (4). However, the biological significance of CRT expression levels in cardiomyocytes under oxidative stress has not been revealed to date.

In the present study, we have investigated the biological role of CRT using rat myocardiac H9c2 cells transfected with the *CRT* gene. We show that the level of CRT alters the sensitivity to apoptosis under oxidative stress with H_2O_2 through a change in Ca^{2+} homeostasis and Ca^{2+}-dependent signaling of the calpain-caspase-12 pathway in myocardiac cells.

MATERIALS AND METHODS

Materials. Antibodies against CRT, calnexin (CNX), binding protein (BiP; glucose-regulating protein 78, Grp78), and ER-specific protein 57 (ERp57)/Grp58 were purchased from Stressgen (Victoria,

Address for reprint requests and other correspondence: Y. Ihara, Dept. of Biochemistry and Molecular Biology in Disease, Atomic Bomb Disease Institute, Nagasaki Univ. Graduate School of Biomedical Sciences, 1-12-4 Sakamoto, Nagasaki 852-8523, Japan (e-mail: y-ihara@net.nagasaki-u.ac.jp).

The costs of publication of this article were defrayed in part by the payment of page charges. The article must therefore be hereby marked "*advertisement*" in accordance with 18 U.S.C. Section 1734 solely to indicate this fact.

BC, Canada). Antibodies against GAPDH, caspase-12, and caspase-3 were obtained from Chemicon International (Temecula, CA), MoBiTec (Gottingen, Germany), and Cell Signaling Technology (Beverly, MA), respectively. Peroxidase-conjugated secondary antibodies against IgG of rabbit and mouse were purchased from Dako (Glostrup, Denmark). The other reagents used in the study were all of high grade and were obtained from Sigma or Wako Pure Chemicals (Osaka, Japan).

Cell lines and culture. H9c2 cells, a clonal cell line derived from embryonic rat heart, were obtained from the American Type Culture Collection (no. CRL-1446). H9c2 cells that had been transfected with the expression vector for mouse *CRT* cDNA were described previously (24). Two cell lines (CRT-S2 and CRT-S8) expressing high levels of CRT protein were used in the study. A 0.6-kb restriction fragment with *Eco*RI containing the translation initiation site was cut from the vector pcDNA3.1/mCRT (24) and inserted in the reverse orientation into pcDNA3.1 (Invitrogen) to obtain antisense CRT (20). The antisense cDNA expression vector was also transfected into H9c2 cells to establish a cell line (CRT-AS) in which the expression of *CRT* was suppressed (20). The established cell lines were used between *passages 12* and *18*. Cells were cultured in DMEM supplemented with 10% FCS in a humidified atmosphere of 95% air-5% CO_2 at 37°C. To induce oxidative stress, cells were cultured with media containing different concentrations of H_2O_2.

Immunoblot analysis. Cultured cells were harvested and lysed in lysis *buffer A* (20 mM Tris·HCl, pH 7.2, 130 mM NaCl, and 1% Nonidet P-40) including protease inhibitors (in μM: 20 4-amidinophenylmethanesulfonyl fluoride, 50 pepstatin, and 50 leupeptin). Protein samples were electrophoresed on 10% SDS-polyacrylamide gels under reducing conditions and then transferred onto a nitrocellulose membrane as described previously (19). The membrane was blocked with 5% skim milk in Tris-buffered saline (TBS; in mM: 10 Tris·HCl, pH 7.5, and 150 NaCl) and then incubated at 4°C overnight with primary antibody in TBS containing 0.05% Tween 20. The blots were coupled with the peroxidase-conjugated secondary antibodies, washed, and then developed using the ECL detection kit (Amersham Biosciences) according to the manufacturer's instructions. The intensity of protein bands was quantified densitometrically, and the value was estimated relative to that for GAPDH.

Fluorescence microscopy. Cells (50,000/ml) were grown on Lab-Tek chamber slides (Nunc) for 24 h. They were fixed with 4% paraformaldehyde in PBS (pH 7.2) and permeabilized for 10 min with PBS containing 1% Triton X-100. The cells were then blocked with 1% BSA in PBS, incubated with the antibody for 1 h, and washed with PBS containing 1% BSA. The immunoreactive primary antibodies were visualized using FITC-conjugated anti-rabbit immunoglobulins (Cappel). After being washed, the stained cells were mounted in VectaShield medium. A Zeiss Axioskop2 (Zeiss, Jena, Germany) with illumination for epifluorescence was used for fluorescence microscopic analysis.

Cell viability assay. The viability of cultured cells was evaluated by performing a 3-(4,5-dimethylthiazol-2-yl)-2,5-diphenyltetrazolium bromide (MTT) assay as described previously (38). Cells (5,000–10,000) were placed into 100 μl of medium per well in 96-well plates and cultured overnight. After cells were treated with H_2O_2, 10 μl of 0.5% MTT solution was added and the cells were incubated for 4 h. The reaction was stopped by adding 100 μl of lysis *buffer B* (20% SDS and 50% *N,N*-dimethyl formamide, pH 4.7), and then cell viability was evaluated by measuring the absorbance at 570 nm using a microplate reader.

Lactate dehydrogenase release assay. After H_2O_2 treatment, the incubation medium was collected and centrifuged at 10,000 *g* for 20 min, and the supernatant was stored at 4°C for the lactate dehydrogenase (LDH) activity assay. In untreated cells, the medium was removed and the same volume of lysis *buffer A* was added to the cells. The cells were lysed by trituration and centrifuged as described above, and then the supernatant was used to assay the LDH activity of all cells. LDH activity was measured spectrophotometrically using an LDH assay kit (MTX "LDH"; Kyokuto Pharmaceutical, Tokyo, Japan) according to the manufacturer's instructions.

Apoptosis assay. Apoptosis was detected by performing flow cytometry using the terminal deoxynucleotidyltransferase-mediated dUTP nick-end labeling (TUNEL) method (11) with the ApopTag Plus fluorescein in situ apoptosis detection kit (Chemicon International) as described previously (56). Morphological changes of nuclei in apoptotic cells were also characterized using fluorescence microscopy. Cells (50,000/ml) were grown on Lab-Tek chamber slides for 24 h. After undergoing H_2O_2 treatment, cells were fixed with 4% paraformaldehyde in PBS. The cells were stained with 2 μg/ml Hoechst 33342 (Molecular Probes, Eugene, OR) in PBS for 5 min so that we could visualize the nuclei. After being rinsed with PBS, the slides were examined using fluorescence microscopy as described above.

Measurement of cytoplasmic free Ca^{2+}. $[Ca^{2+}]_i$ was measured using a dual-excitation wavelength spectrofluorophotometer (RF-5500; Shimadzu, Kyoto, Japan) with fura-2 essentially as described previously (6, 36), but with a slight modification. Briefly, cultured cells on glass coverslips were loaded with 5 μM fura-2 AM (Dojindo, Kumamoto, Japan) for 20 min in Earle's balanced salt solution (EBSS; in mM: 26 $NaHCO_3$, pH 7.4, 1 NaH_2PO_4, 5.4 KCl, 116 NaCl, 5.5 glucose, and 2 $CaCl_2$) in the presence of 0.01% Pluronic acid F-127. After being washed four times with EBSS, the coverglass was positioned at a 45° angle to both excitation and emission light paths in a quartz cuvette containing 3.5 ml of fresh EBSS. Fura-2 fluorescence was determined at 37°C using the spectrofluorophotometer operating at an emission wavelength of 505 nm and excitation wavelengths of 340 and 380 nm. The maximal signal (R_{max}) was obtained by adding ionomycin at a 4 μM final concentration. Subsequently, the minimal signal (R_{min}) was obtained by adding EGTA at a 10 mM final concentration, followed by Tris-free base to a 30 mM final concentration, to increase the pH to 8.3. R is the ratio (F_1/F_2) of the fluorescence of excitation at 340 nm and emission at 505 nm (F_1) to that of excitation at 380 nm and emission at 505 nm (F_2). The actual $[Ca^{2+}]$ was calculated as $K_d \times (R - R_{min})/(R_{max} - R) \times Sf2/Sb2$, with K_d = 224 nM (16). The Sf2-to-Sb2 ratio is the ratio of fura-2 fluorescence at 380 nm in Ca^{2+}-free medium to that in Ca^{2+}-replete medium.

Assays for uptake and release of Ca^{2+} in the cell. The uptake of Ca^{2+} was measured radiometrically using the Millipore filtration technique as described previously (49), with a slight modification. The cells were cultured with the medium containing H_2O_2 for the periods indicated and then washed with EBSS and cultured for 10 min in EBSS containing $^{45}Ca^{2+}$ (5 μCi/ml). Cells were detached from the culture wells using trypsinization buffer (0.25% trypsin and 0.02% EDTA in EBSS), and the cell suspension was filtered through a 0.45-μm nitrocellulose filter (Bio-Rad Laboratories, Hercules, CA) under vacuum conditions. The filters were rinsed twice with 0.5 ml of washing buffer (in mM: 10 HEPES, pH 7.4, 150 KCl, 2 EGTA, and 2.5 $MgCl_2$). $^{45}Ca^{2+}$ uptake was calculated by measuring radioactivity and standardized according to protein concentrations. For the $^{45}Ca^{2+}$ release assay, cells were cultured for 48 h with the medium containing $^{45}Ca^{2+}$ (1 μCi/ml). After being washed with EBSS, the cells were incubated with EBSS containing H_2O_2. Aliquots were collected at the time points indicated and centrifuged. The radioactivity was measured in the supernatant as the amount of Ca^{2+} released from the cell.

Enzyme assay. Caspase-12 activity was measured with Ala-Thr-Ala-Asp-7-amino-4-trifluoromethylcoumarin (AFC) as a substrate by using a caspase-12 fluorometric assay kit (BioVision, Mountain View, CA) according to the manufacturer's protocol. The assay is based on the detection of cleavage of the substrate, and the activity was quantified using a spectrofluorophotometer to measure fluorescence (excitation, 400 nm; emission, 505 nm) derived from free AFC. Calpain activity was measured using the calpain substrate succinyl-Leu-Leu-Val-Tyr-7-amino-4-methylcoumarin (Suc-Leu-Leu-Val-Tyr-AMC) as described by Glading et al. (13), with a slight modification.

Cultured cells were treated with or without H_2O_2 and/or thapsigargin and then harvested and washed with EBSS. Cells were resuspended in EBSS at 2.5×10^5 cells/ml and kept on ice for up to 1 h. In each sample, 250 μl were added to a 2.5-ml quartz cuvette with stirring and allowed to warm to 37°C in the spectrofluorophotometer. At time −1 min, ionomycin in DMSO was added to a final 2.5 μM concentration. DMSO alone was added as a control. At *time 0*, Suc-Leu-Leu-Val-Tyr-AMC was added to a final 50 μM concentration, and fluorescence (excitation, 360 nm; emission, 460 nm) was measured immediately for 3 min.

Statistical analysis. Statistical analysis was performed as previously recommended (6a) using Student's *t*-test or ANOVA (StatView software). Significance was set at $P < 0.05$.

RESULTS

Overexpression of CRT enhances cytotoxic sensitivity of H9c2 cells to oxidative stress caused by H_2O_2. Rat myocardiac H9c2 cells were transfected with the expression vector for mouse *CRT* cDNA to obtain cell lines overexpressing CRT (24). Figure 1*A* shows that the expression of CRT increased in the overexpressed cells to ~2.7-fold the level in the parental and mock-transfected (control) H9c2 cells. The transfection had no apparent effect on the expression of other ER proteins such as CNX, BiP, and ERp57. The intracellular localization of CRT was examined using indirect immunofluorescence. As shown in Fig. 1*B*, immunoreactive signals showed a perinuclear reticular pattern in all cases, including the control and CRT-overexpressing cells, although the signal intensity was increased in the transfectants compared with the control cells. To investigate the effect of overexpression of CRT on the cytotoxic sensitivity of H9c2 cells to oxidative stress, control and CRT-overexpressing cells were exposed to different concentrations of H_2O_2 for 1 h and then cell viability was examined by performing an MTT assay as described in MATERIALS AND METHODS. One hour of exposure to H_2O_2 caused cell damage in a dose-dependent manner, and the cytotoxic effect was enhanced more in the gene-transfected cells (i.e., CRT-S2 and CRT-S8) than in the controls (i.e., parental and control vector-transfected cells) (Fig. 2*A*, *left*). As shown in Fig. 2*A*, *right*, in CRT-overexpressing cells, the cell viability was markedly reduced after 1-h exposure to 50 μM H_2O_2, although less reduction was observed in control cells. However, in both control and gene-transfected cells, viability was similarly suppressed after 4 h of exposure to 50 μM H_2O_2. Next, control and CRT-overexpressing cells were exposed to different concentrations of H_2O_2 for 2 h, and then the cytotoxic effect of H_2O_2 was examined by assaying LDH release as described in MATERIALS AND METHODS. Two hours of exposure to H_2O_2 caused cell damage in a dose-dependent manner, and the cytotoxic effect was enhanced more in the gene-transfected cells than in the controls (Fig. 2*B*, *left*). In Fig. 2*B*, *right*, the cells were treated with 50 μM H_2O_2 for the periods indicated, and the LDH released into the medium was quantified and expressed as a ratio to the total intracellular LDH content. The LDH release was enhanced more in the gene-transfected cells than in the controls during the treatment. Figure 2*C* shows that morphological change was observed using phase-contrast microscopy in control and CRT-overexpressing cells treated with 50 μM H_2O_2 for 2 h. In gene-transfected cells treated with H_2O_2, the cell shape was apparently round and had shrunk along with some bleblike structure, although no change was observed in control cells treated with H_2O_2. Collectively, these results indicate that overexpression of CRT enhances the cytotoxic sensitivity to oxidative stress caused by H_2O_2 in myocardiac H9c2 cells.

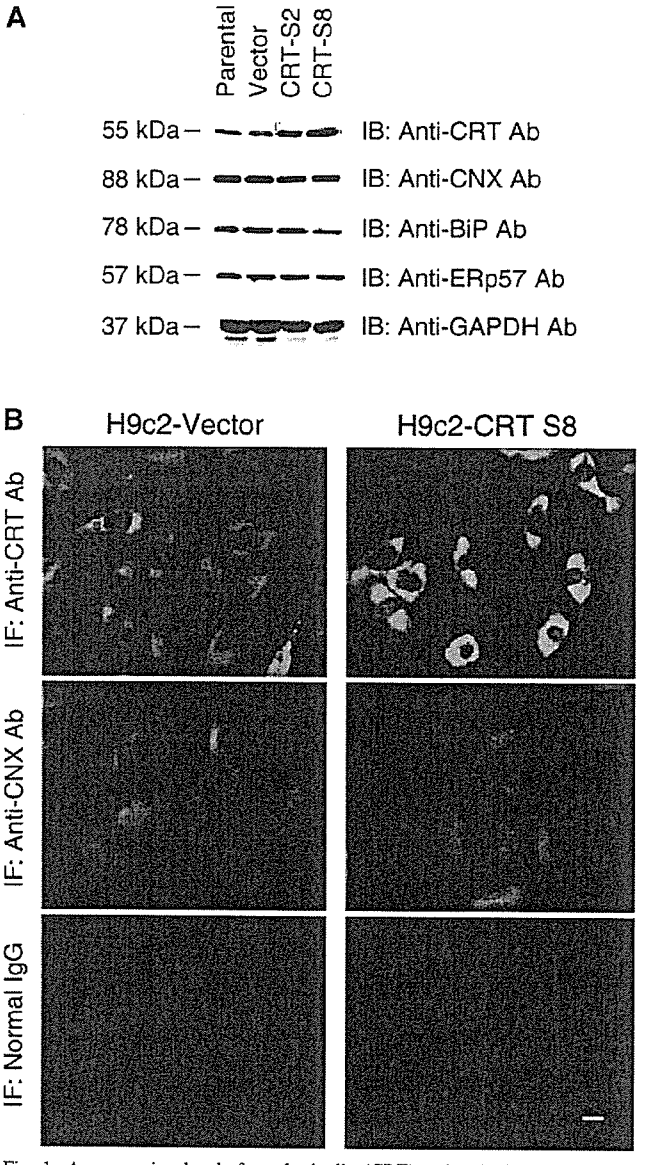

Fig. 1. *A*: expression levels for calreticulin (CRT), calnexin (CNX), binding protein (BiP; glucose-regulating protein 78, Grp78), ERp57/Grp58, and GAPDH were estimated in control (parental and vector) and *CRT* gene-transfected H9c2 (CRT-S2 and CRT-S8) cells using immunoblot analysis with specific antibodies (Ab) as described in MATERIALS AND METHODS. Data represent 3 independent experiments. *B*: intracellular localization of CRT and CNX was evaluated in control and *CRT* gene-transfected H9c2 cells using indirect immunofluorescence (IF) microscopy with specific antibodies. Background signals were obtained in cells stained with normal rabbit IgG. Data represent 3 independent experiments. Bar, 10 μm.

Overexpression of CRT enhances apoptosis of H9c2 cells under oxidative stress due to H_2O_2. To examine whether apoptosis contributed to the cell damage observed in the transfectants under oxidative stress, a TUNEL assay was performed using cells treated with H_2O_2. In the study by Turner et

al. (52), maximal fragmentation of DNA was observed in H9c2 cells treated with 250 μM H_2O_2 for 4 h. We compared the extent of DNA strand breaks between control and gene-transfected cells treated with 50 μM H_2O_2 for 1 and 4 h. The TUNEL assay (Fig. 3*A*) showed that an increase in fluorescence intensity derived from DNA strand breaks in the transfectants but not in the control cells after H_2O_2 treatment. After the nucleus was stained with Hoechst 33342

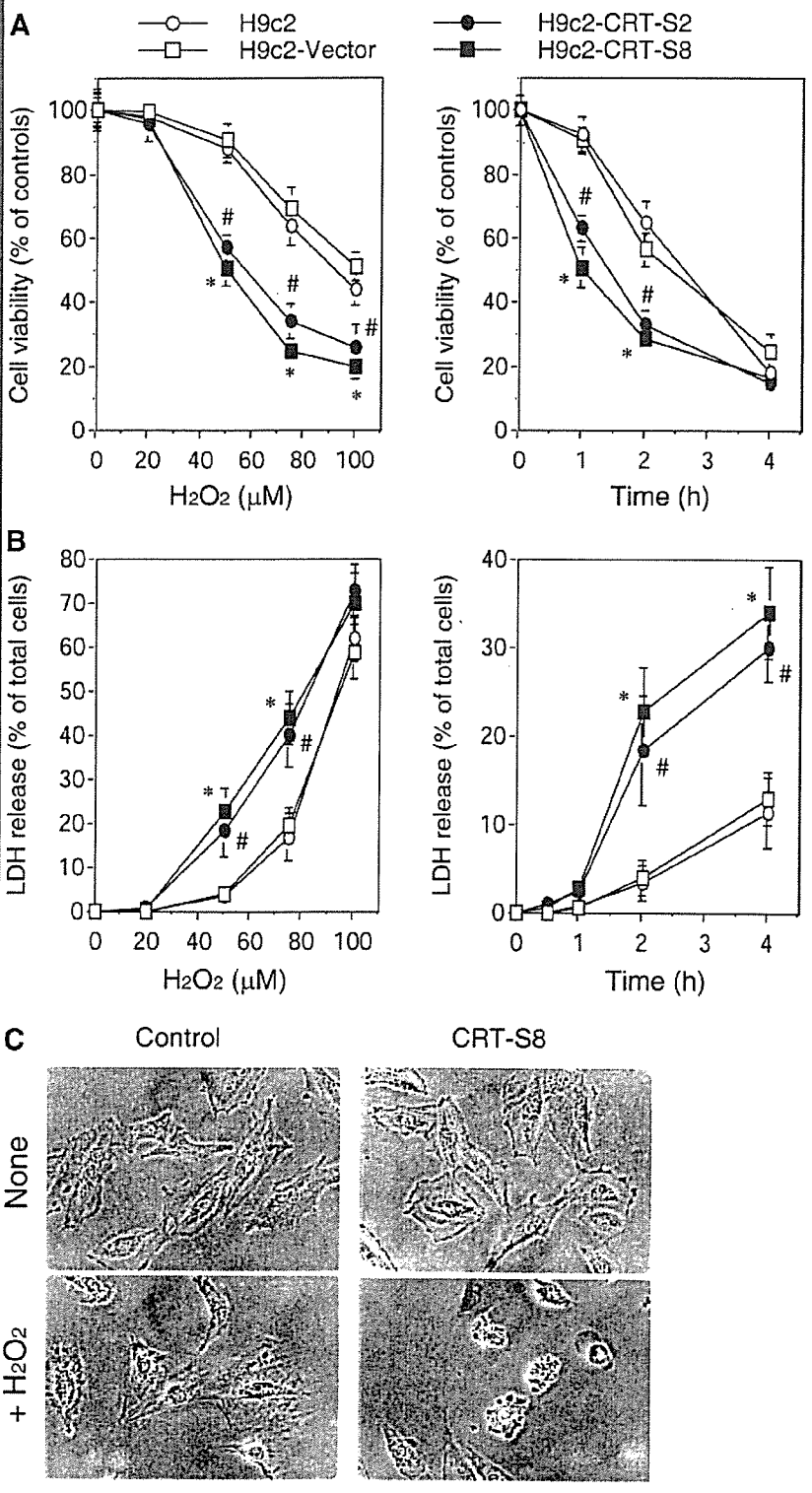

Fig. 2. Overexpression of CRT promotes cell damage in H9c2 cells under oxidative stress due to H_2O_2. *A*: control (H9c2 and H9c2-Vector) and *CRT* gene-transfected (H9c2-CRT-S2 and H9c2-CRT-S8) cells were exposed to different concentrations of H_2O_2 for 1 h, and then cell viability was examined by performing a 3-(4,5-dimethylthiazol-2-yl)-2,5-diphenyltetrazolium bromide (MTT) assay as described in MATERIALS AND METHODS (*left*). Cells were exposed to 50 μM H_2O_2 for the periods indicated, and then cell viability was examined by performing an MTT assay (*right*). Each value represents the mean ± SD of 4–6 independent experiments. Statistical analysis was performed using a factorial ANOVA test. $*P < 0.05$, $\#P < 0.05$ vs. value at same H_2O_2 concentration (*left*) or time point (*right*) for H9c2 cells treated with H_2O_2. *B*: control and *CRT* gene-transfected cells were exposed to different concentrations of H_2O_2 for 2 h, and then cell damage was examined by performing a lactate dehydrogenase (LDH) release assay as described in MATERIALS AND METHODS (*left*). Cells were treated with 50 μM H_2O_2 for the periods indicated, and the LDH released in the medium was quantified as described in MATERIALS AND METHODS and expressed as a percentage of total intracellular LDH content (*right*). Each value represents the mean ± SD of 4–6 independent experiments. $*P < 0.05$, $\#P < 0.05$ vs. value at same H_2O_2 concentration (*left*) or time point (*right*) as H9c2 cells treated with H_2O_2. *C*: control (H9c2-Vector), *CRT* gene-transfected (H9c2-CRT-S8) cells were exposed to 50 μM H_2O_2 for 2 h, and then cell morphology was examined using phase-contrast microscopy. Bar, 10 μm.

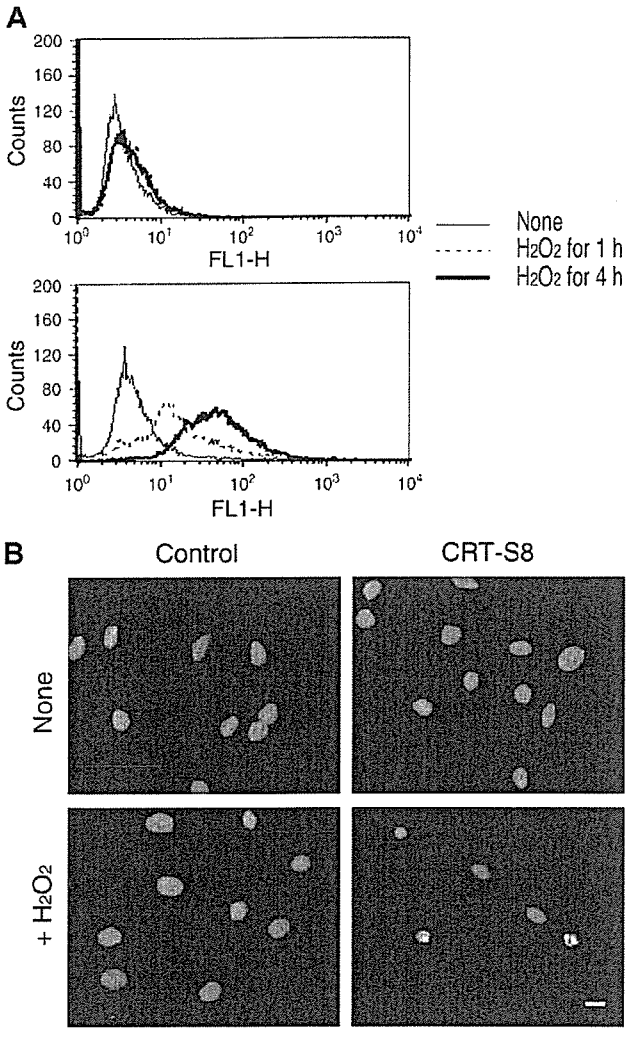

Fig. 3. Overexpression of CRT promotes apoptosis in H9c2 cells under oxidative stress due to H_2O_2. *A*: terminal deoxynucleotidyltransferase-mediated dUTP nick-end labeling (TUNEL) assay was performed for control (*top*) and gene-transfected (*bottom*) H9c2 cells under oxidative stress caused by H_2O_2. DNA strand breaks were detected using the TUNEL method as described in MATERIALS AND METHODS. Cells were treated with 50 μM H_2O_2 for the periods indicated. Data represent 3 independent experiments. *B*: morphological changes to nuclei were characterized in Hoechst-stained cells using a fluorescence microscope. Control and gene-transfected cells (50,000/ml) were grown on Lab-Tek chamber slides for 24 h and then treated with 50 μM H_2O_2 for 2 h. After being fixated with 4% paraformaldehyde in PBS, cells were stained with Hoechst 33342 and then visualized using fluorescence microscopy as described in MATERIALS AND METHODS. Bar, 10 μm.

(Fig. 3*B*), chromatin condensation and nuclear fragmentation were observed in the gene-transfected cells treated with H_2O_2, but not in the control cells treated with H_2O_2. Altogether, these results indicate that overexpression of CRT significantly enhances apoptosis in H9c2 cells under oxidative stress caused by H_2O_2.

Overexpression of CRT increases $[Ca^{2+}]_i$ in H9c2 cells under oxidative stress due to H_2O_2. To investigate whether the intracellular Ca^{2+} homeostasis was affected in the cells under oxidative stress, we measured $[Ca^{2+}]_i$ after H_2O_2 treatment (50 or 75 μM). To observe the effect of extracellular Ca^{2+} on $[Ca^{2+}]_i$, we treated the cells with H_2O_2 in the presence of 2 mM Ca^{2+} (+Ca^{2+}) or 10 mM EGTA (+EGTA). The measurement was based on the fluorescence intensity of cells loaded with fura-2 AM as described in MATERIALS AND METHODS. Figure 4 shows that in the presence of extracellular Ca^{2+} (+Ca^{2+}), control cells demonstrated no change in $[Ca^{2+}]_i$ level during treatment with 50 μM H_2O_2, but CRT-overexpressing cells increased to 180 nM after 35 min of treatment. Moreover, with 75 μM H_2O_2 treatment, the difference in the $[Ca^{2+}]_i$ increase was greater. On the other hand, in the absence of extracellular Ca^{2+} (+EGTA), the H_2O_2-induced $[Ca^{2+}]_i$ increase was not observed even in the CRT-overexpressing cells, suggesting that the increase was dependent on the influx of Ca^{2+} from the extracellular space. Altogether, the results indicate that $[Ca^{2+}]_i$ was apparently increased by oxidative stress due to H_2O_2 in CRT-overexpressing cells compared with controls, suggesting some modification of cellular Ca^{2+} homeostasis occurred because of CRT overexpression.

Alteration of Ca^{2+} flux in CRT-overexpressing H9c2 cells under oxidative stress. To investigate the effect of overexpression of CRT on Ca^{2+} influx in cells under oxidative stress, we examined the $^{45}Ca^{2+}$ uptake in control and *CRT* gene-trans-

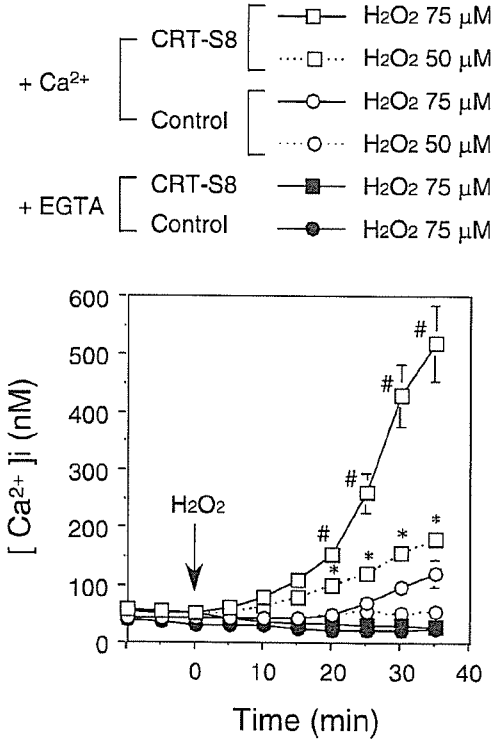

Fig. 4. Cytoplasmic free Ca^{2+} concentration ($[Ca^{2+}]_i$) increases in CRT-overexpressing H9c2 cells under oxidative stress due to H_2O_2. After being loaded with 5 μM fura-2 AM, control and gene-transfected cells cultured on glass coverslips were treated with H_2O_2 (50 or 75 μM) for the periods indicated. $[Ca^{2+}]_i$ was quantified by measuring fura-2 fluorescence as described in MATERIALS AND METHODS. To observe the effect of extracellular Ca^{2+} on $[Ca^{2+}]_i$, we treated the cells with H_2O_2 in the presence of 2 mM Ca^{2+} (+Ca^{2+}) or 10 mM EGTA (+EGTA). Each value represents the mean ± SD of 4 independent experiments. Statistical analysis was performed using a factorial ANOVA test. $^*P < 0.05$ vs. value at same time point for control cells (Ca^{2+}) treated with 50 μM H_2O_2. #$P < 0.05$ vs. value at same time point for control cells (Ca^{2+}) treated with 75 μM H_2O_2.

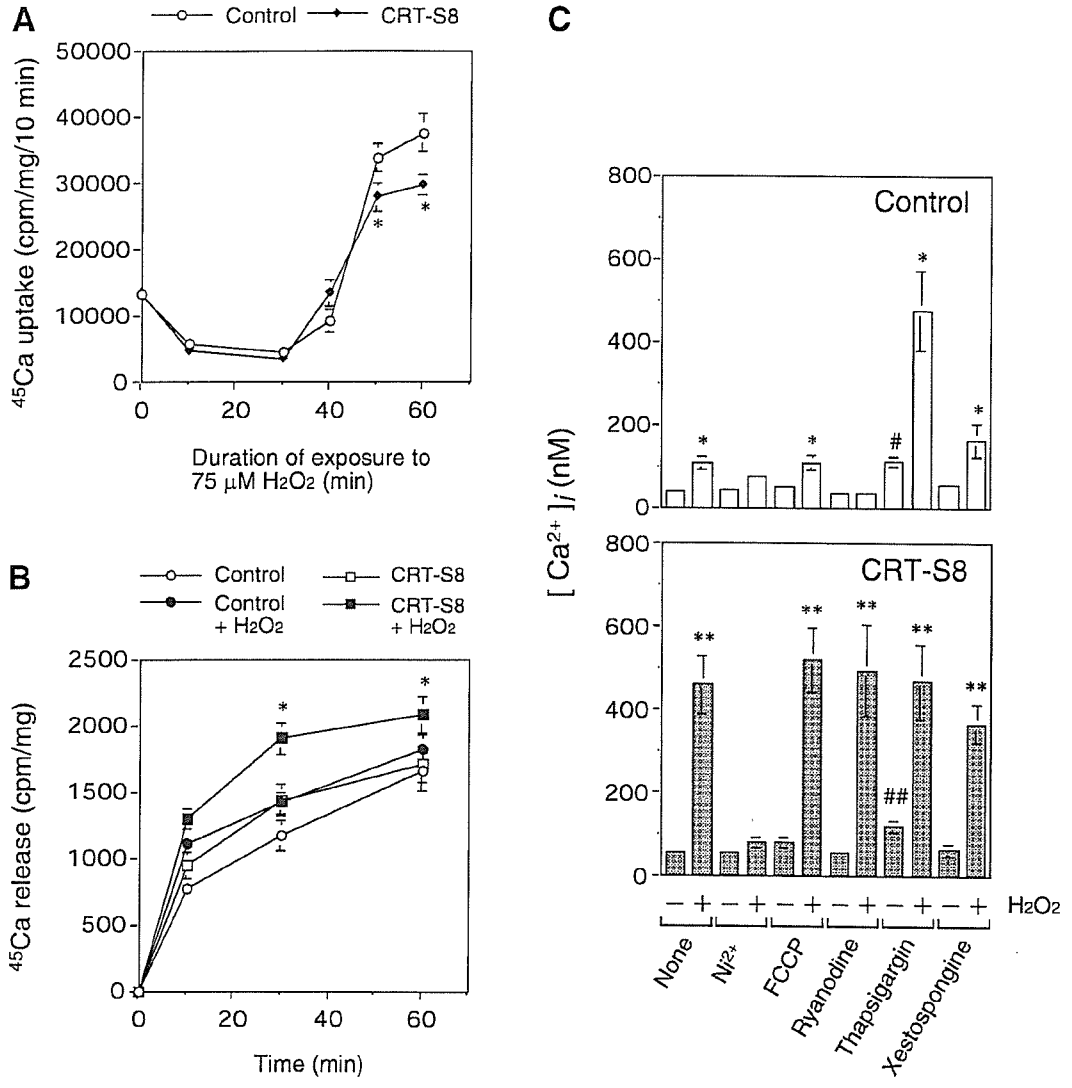

Fig. 5. *A*: uptake of Ca^{2+} in CRT-overexpressing H9c2 cells under oxidative stress due to H_2O_2. The cells were cultured with the medium containing 75 μM H_2O_2 for the indicated periods, washed with Earle's balanced salt solution (EBSS), and then cultured for 10 min in EBSS containing $^{45}Ca^{2+}$ (5 μCi/ml) as described in MATERIALS AND METHODS. After being washed with EBSS, the cells were harvested and $^{45}Ca^{2+}$ uptake was measured as described in MATERIALS AND METHODS. Each value represents mean ± SD of 3 independent experiments. Statistical analysis was performed using a factorial ANOVA test. $*P < 0.05$ compared with value at same time point for control cells treated with 75 μM H_2O_2. *B*: release of Ca^{2+} from CRT-overexpressing H9c2 cells under oxidative stress due to H_2O_2. Cells were cultured for 48 h with $^{45}Ca^{2+}$ as described in MATERIALS AND METHODS. After being washed with EBSS, the cells were incubated with EBSS containing 75 μM H_2O_2. Aliquots were collected at the time points indicated and then centrifuged. Radioactivity was measured in the supernatant as the amount of Ca^{2+} released from the cell. Each value represents mean ± SD of counts per minute (cpm) recovered in the supernatant normalized to the protein in the total cell pellets. $*P < 0.05$ vs. same time point for CRT-S8 cells treated without H_2O_2. *C*: effect of Ca^{2+} modulators on $[Ca^{2+}]_i$ in CRT-overexpressing H9c2 cells under oxidative stress with H_2O_2. After being loaded with 5 μM fura-2 AM, control and gene-transfected cells cultured on glass coverslips were pretreated with various modulators containing Ni^{2+} (5 mM), FCCP (1 μM), ryanodine (100 μM), thapsigargin (5 μM), and xestospongin C (1 μM) and then were treated with H_2O_2 (75 μM) for 30 min. $[Ca^{2+}]_i$ was quantified by measuring fura-2 fluorescence as described in MATERIALS AND METHODS. Each value represents mean ± SD of 3 independent experiments. $*P < 0.05$ vs. corresponding control cells treated without H_2O_2. $\#P < 0.05$ vs. untreated control cells (None). $**P < 0.05$ vs. corresponding CRT-S8 cells treated without H_2O_2. $\#\#P < 0.05$ vs. untreated CRT-S8 cells (None).

fected cells during treatment with 75 μM H_2O_2 as described in MATERIALS AND METHODS. As shown in Fig. 5*A*, in both control and gene-transfected cells, the rate of $^{45}Ca^{2+}$ uptake was suppressed within the first 30 min and then increased during oxidative stress. The uptake rate was higher in the control than in the gene-transfected cells after 40 min. Next, to investigate the effect of overexpression of CRT on Ca^{2+} efflux in the cell under oxidative stress, we examined the $^{45}Ca^{2+}$ release in control and gene-transfected cells during treatment with 75 μM H_2O_2 as described in MATERIALS AND METHODS. After being labeled with $^{45}Ca^{2+}$, the cells were treated with H_2O_2 and the amount of $^{45}Ca^{2+}$ released was measured as described in MATERIALS AND METHODS. As shown in Fig. 5*B*, although the amount of $^{45}Ca^{2+}$ released did not differ between untreated control and gene-transfected cells, the release was increased in gene-transfected cells compared with controls after 30-min treatment with H_2O_2. Collectively, in CRT-overexpressing cells, Ca^{2+} influx seemed to be suppressed and the efflux was

increased in the cells under oxidative stress caused by H_2O_2 compared with control cells treated with H_2O_2. Although these results were not consistent with the finding that $[Ca^{2+}]_i$ was highly elevated in gene-transfected cells treated with H_2O_2 (Fig. 4), they also suggested that an alteration of responses in the intracellular Ca^{2+} stores might lead to increased $[Ca^{2+}]_i$ in CRT-overexpressing cells.

Effect of Ca^{2+} modulators on $[Ca^{2+}]_i$ in CRT gene-transfected H9c2 cells under oxidative stress due to H_2O_2. To investigate whether intracellular Ca^{2+} pools contribute to the altered Ca^{2+} homeostasis, we examined the effect of Ca^{2+} modulators on $[Ca^{2+}]_i$ in cells treated with H_2O_2 (Fig. 5*C*). Ni^{2+} (5 mM) was used to block Ca^{2+} influx from the extracellular space via Ca^{2+} channels and Na^+/K^+ exchangers in the plasma membrane (26, 27). FCCP (1 μM) is a mitochondrial uncoupler that collapses the mitochondrial membrane potential that drives Ca^{2+} uptake into mitochondria (5). A high concentration of ryanodine (100 μM) was used as an antagonist for the ryanodine receptor (55). Thapsigargin (5 μM) was used to inhibit the function of sarco(endo)plasmic reticulum Ca^{2+}-ATPase (SERCA) to block the uptake of Ca^{2+} into the ER/sarcoplasmic reticulum (SR) (50). Xestospongin C (1 μM) is a cell-permeable inhibitor of the inositol 1,4,5-trisphosphate (IP_3) receptor (10). The cells were treated with each Ca^{2+} modulator for 10 min after being loaded with fura-2 AM and then were incubated with 75 μM H_2O_2 for 30 min, and $[Ca^{2+}]_i$ was measured as described in MATERIALS AND METHODS. The uptake of Ca^{2+} into mitochondria and the ER was disrupted by treatment with FCCP and thapsigargin, respectively. In control cells, FCCP did not enhance the H_2O_2-induced increase of $[Ca^{2+}]_i$. In CRT-overexpressing cells, $[Ca^{2+}]_i$ was similarly increased by H_2O_2 both cases, with and without FCCP. These results indicate no influence of FCCP on the H_2O_2-induced change of $[Ca^{2+}]_i$ in control and CRT-overexpressing cells. This finding also suggests that the enhancement of H_2O_2-induced increase of $[Ca^{2+}]_i$ observed in CRT-overexpressing cells may not be explained solely by dysfunction of mitochondrial Ca^{2+} uptake. In contrast, the H_2O_2-induced increase in $[Ca^{2+}]_i$ was apparently enhanced in control cells treated with thapsigargin. This indicates that the thapsigargin-sensitive pool (i.e., ER) is involved in the enhancement of H_2O_2-induced increase of $[Ca^{2+}]_i$ and also suggests that dysfunction of SERCA may have a promoting effect on the H_2O_2-induced increase of $[Ca^{2+}]_i$. The ryanodine and IP_3 receptors may be involved in the increase in $[Ca^{2+}]_i$ in response to H_2O_2. However, high concentrations of ryanodine and xestospongin C did not suppress the increase in $[Ca^{2+}]_i$ in CRT-overexpressing cells treated with H_2O_2, suggesting that the ryanodine and IP_3 receptors were not necessarily the main sources of the H_2O_2-induced increase of $[Ca^{2+}]_i$ in CRT-overexpressing cells. Furthermore, it was noteworthy that the H_2O_2-induced increase of $[Ca^{2+}]_i$ was clearly suppressed by Ni^{2+} in gene-transfected cells. This finding is also consistent with the result that the increase was inhibited in gene-transfected cells in the absence of extracellular Ca^{2+} (Fig. 4). These findings indicate that the influx of Ca^{2+} from the extracellular space is important for the H_2O_2-induced increase of $[Ca^{2+}]_i$ in CRT-overexpressing cells, despite the fact that the rate of influx was not increased in the gene-transfected cells treated with H_2O_2 (Fig. 5*A*). Altogether, these results indicate that the ER-stored Ca^{2+} pool plays an important role in the enhancement of the H_2O_2-induced increase of $[Ca^{2+}]_i$ in CRT-overexpressing cells, although Ca^{2+} influx from the extracellular space was also an important contributor to the increase.

$[Ca^{2+}]_i$ level is implicated in the susceptibility of H9c2 cells to apoptosis under oxidative stress due to H_2O_2. To determine whether the increase in $[Ca^{2+}]_i$ is part of the causative mechanism of apoptosis in the gene-transfected cells, H_2O_2-dependent cytotoxicity was examined in CRT-overexpressing cells in the presence or absence of BAPTA-AM, a cell-permeable Ca^{2+} chelator. As shown in Fig. 6*A*, *top*, cell viability was assessed by performing an MTT assay in gene-transfected cells exposed to H_2O_2 treatment (50 μM for 2 h) in the absence or presence of BAPTA-AM (10 μM). The viability was suppressed by H_2O_2 to 28.0 ± 3.4% of that in untreated cells in the absence of BAPTA-AM but returned to 50.5 ± 6.5% in its presence. As shown in Fig. 6*A*, *bottom*, cell damage was also assessed by performing a LDH release assay in gene-transfected cells exposed to H_2O_2 treatment (50 μM for 2 h) in the absence or presence of BAPTA-AM. The release was increased by H_2O_2 to 22.0 ± 5.4% that of untreated cells in the absence of BAPTA-AM but was remitted to 4.7 ± 2.5% in its presence. These results suggest that BAPTA-AM mitigates cell damage due to H_2O_2 by suppressing the increase of $[Ca^{2+}]_i$. The effect of BAPTA-AM on apoptosis was also examined using the TUNEL method in the gene-transfected cells after H_2O_2 treatment (Fig. 6*B*). In the absence of BAPTA-AM, TUNEL-positive cells increased after treatment with 50 μM H_2O_2 for 2 h but were not detected in the presence of BAPTA-AM even 2 h after treatment with H_2O_2. Conversely, the effect of an $[Ca^{2+}]_i$ increase on H_2O_2-induced apoptosis was examined in control H9c2 cells in the absence or presence of thapsigargin (5 μM), an inhibitor for SERCA (50). As shown in Fig. 6*C*, *top*, cell viability was suppressed by H_2O_2 (50 μM for 2 h) to 60.0 ± 4.4% of that in untreated cells in the absence of thapsigargin but was suppressed to 17.1 ± 4.6% in its presence. In Fig. 6*C*, *bottom*, cell damage was assessed by performing a LDH release assay in control cells exposed to H_2O_2 treatment (50 μM for 2 h) in the absence or presence of thapsigargin. The release was slightly increased by H_2O_2 to 7.5 ± 2.2% that of untreated cells in the absence of thapsigargin but was enhanced to 32.7 ± 2.5% in its presence. Furthermore, the effect of thapsigargin on apoptosis was examined using the TUNEL method in control cells with H_2O_2 treatment (Fig. 6*D*). In the presence of thapsigargin, TUNEL-positive cells increased in number after exposure to 50 μM H_2O_2 for 2 h, whereas in its absence, no increase was observed. These results suggest that thapsigargin enhances apoptosis caused by H_2O_2 treatment by increasing the $[Ca^{2+}]_i$ level. This finding was also consistent with our recently reported results (56). Altogether, these results indicate that the increase in $[Ca^{2+}]_i$ plays a causative role in the apoptosis of CRT-overexpressing cells under oxidative stress caused by H_2O_2.

Suppression of CRT expression by transfection with antisense CRT gene enhances cytoprotection of H9c2 cells against oxidative stress due to H_2O_2. To confirm whether the expression level of CRT influences susceptibility to oxidant-induced apoptosis in H9c2 cells, we transfected the cells with the antisense *CRT* gene expression vector and a cell line (CRT-AS) in which CRT expression was suppressed to a level lower than that in controls as described in MATERIALS AND METHODS (20). The expression level of CRT was compared with that in control

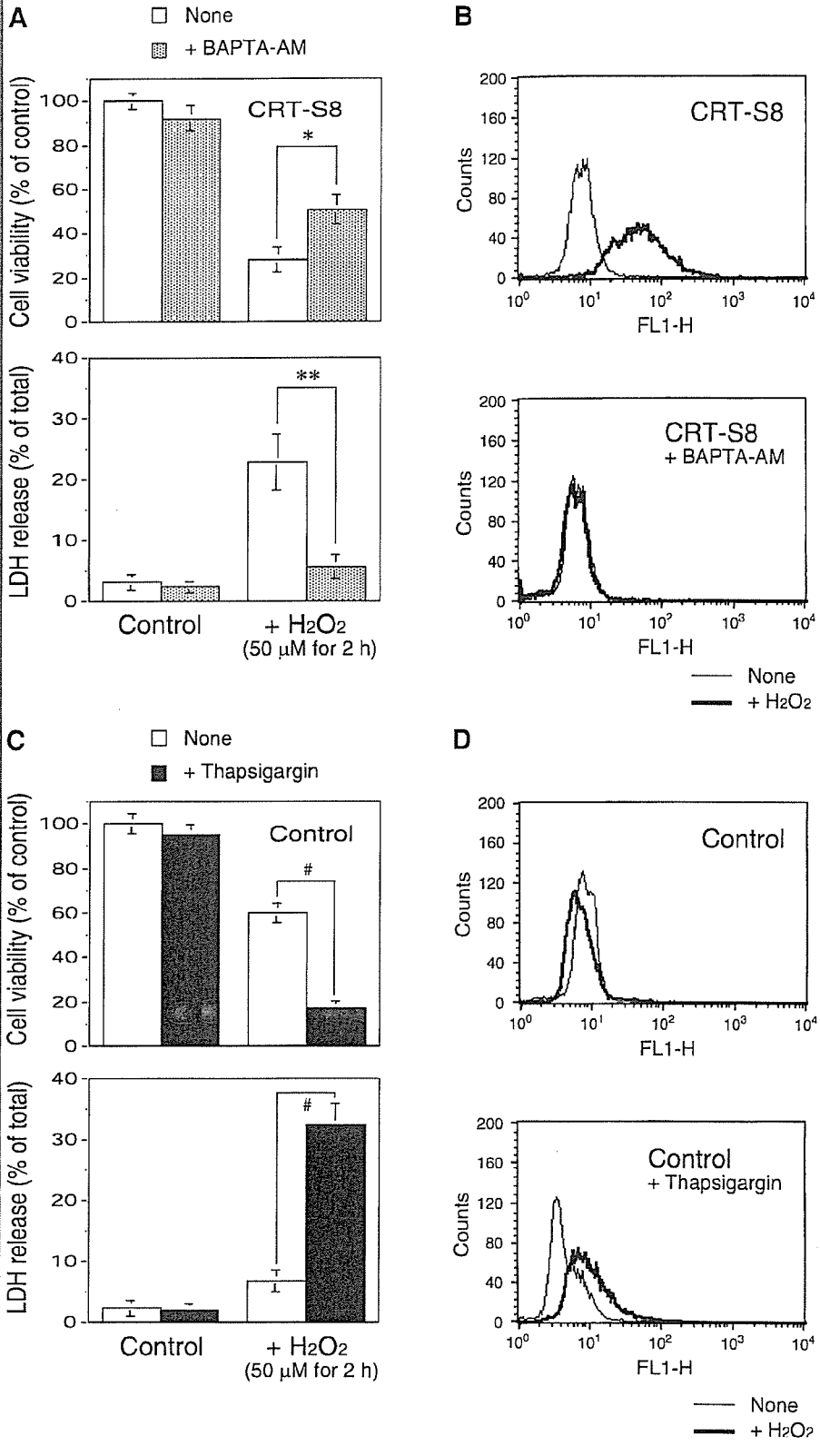

Fig. 6. Effect of Ca^{2+} modulators on apoptosis due to oxidative stress caused by H_2O_2. *A*: CRT-overexpressing (CRT-S8) cells were cultured in the presence or absence of 10 μM BAPTA-AM during the H_2O_2 treatment. The cells were exposed to 50 μM H_2O_2 for 2 h and then cell viability was examined by performing an MTT assay as described in MATERIALS AND METHODS. Each value represents the mean ± SD of 4 independent experiments. Statistical analysis was performed using a paired Student's *t*-test. $*P < 0.05$, $**P < 0.01$ vs. CRT-S8 cells treated with H_2O_2 without BAPTA-AM. *B*: TUNEL assay for CRT-overexpressing cells treated with or without BAPTA-AM and/or H_2O_2. Cells were cultured in the presence or absence of 10 μM BAPTA-AM during the H_2O_2 treatment. Thin line, no H_2O_2 for 2 h; thick line, 50 μM H_2O_2 for 2 h. DNA strand breaks were detected using the TUNEL method as described in MATERIALS AND METHODS. Data represent 3 independent experiments. *C*: control cells were cultured in the presence or absence of 5 μM thapsigargin during the H_2O_2 treatment. Cells were exposed to 50 μM H_2O_2 for 2 h, and then cell viability was examined by performing an MTT assay as described in MATERIALS AND METHODS. Each value represents the mean ± SD of 4 independent experiments. $\#P < 0.01$ vs. control cells treated with H_2O_2 without thapsigargin. *D*: TUNEL assay for control cells treated with or without thapsigargin and/or H_2O_2. Cells were cultured in the presence or absence of 5 μM thapsigargin during H_2O_2 treatment. Thin line, no H_2O_2 for 2 h; thick line, 50 μM H_2O_2 for 2 h. DNA double-stranded breaks were detected using the TUNEL method as described in MATERIALS AND METHODS. Data represent 4 independent experiments.

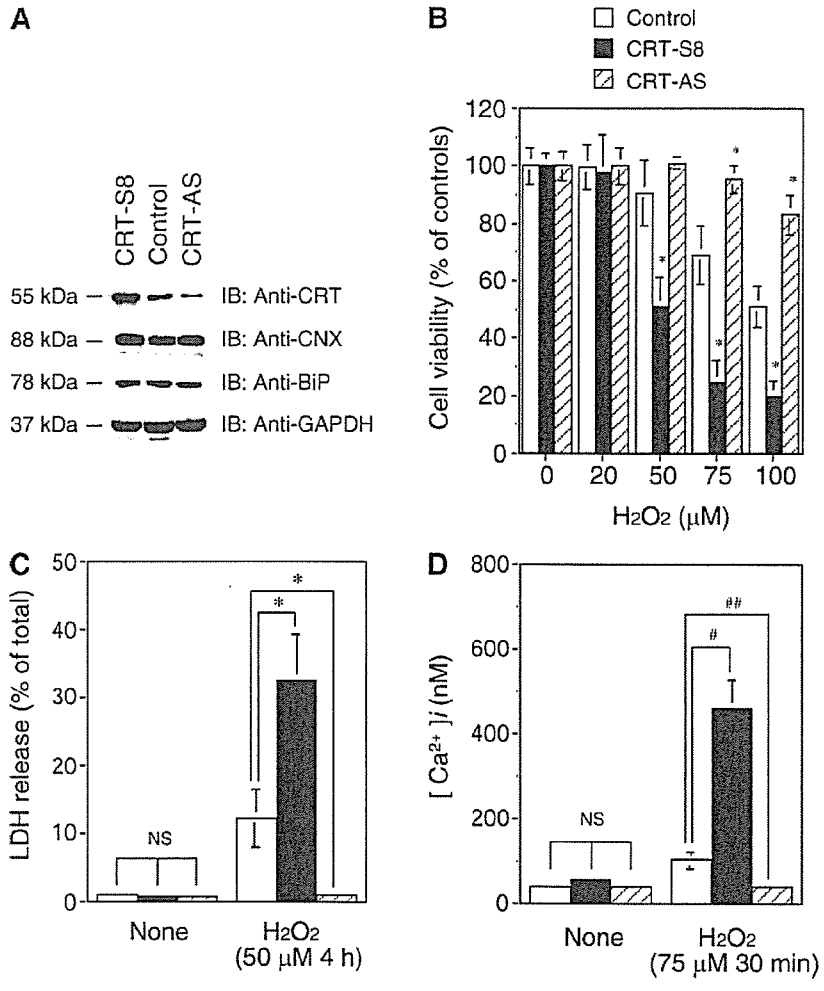

Fig. 7. Suppression of CRT expression showing cytoprotective effects in H9c2 cells under oxidative stress. To observe the effect of the suppressed expression of CRT on cytotoxicity under conditions of oxidative stress, we introduced the antisense gene for CRT into H9c2 cells to obtain cells underexpressing CRT as described in MATERIALS AND METHODS. *A*: expression levels of CRT, CNX, BiP, and GAPDH were examined in control, CRT-overexpressing (CRT-S8), and CRT-underexpressing (CRT-AS) cells using immunoblot analysis with specific antibodies. Data represent 4 independent experiments. *B*: control, CRT-overexpressing, and CRT-underexpressing cells were exposed to different concentrations of H_2O_2 for 1 h, and then cell viability was examined by performing an MTT assay as described in MATERIALS AND METHODS. Each value represents mean ± SD of 4 independent experiments. Statistical analysis was performed using a factorial ANOVA test. $*P < 0.05$ vs. same concentration of H_2O_2 for control cells treated with H_2O_2. *C*: control, CRT-overexpressing, and CRT-underexpressing cells were exposed to 50 μM H_2O_2 for 4 h, and then cell damage was examined by performing an LDH release assay as described in MATERIALS AND METHODS. Each value represents mean ± SD of 4 independent experiments. $*P < 0.01$ vs. control cells treated with H_2O_2. *D*: after being loaded with 5 μM fura-2 AM, control, CRT-overexpressing, and CRT-underexpressing cells cultured on glass coverslips were treated with 75 μM H_2O_2 for 30 min. $[Ca^{2+}]_i$ was quantified by measuring fura-2 fluorescence as described in MATERIALS AND METHODS. $\#P < 0.01$, $\#\#P < 0.05$ vs. control cells treated with H_2O_2.

and CRT-overexpressing cells by immunoblot analysis, and the results showed that the expression level was decreased to ~30% of the control level (Fig. 7*A*). Figure 7*B* shows that control, CRT-overexpressing, and CRT-underexpressing cells were exposed to different concentrations of H_2O_2 for 1 h, and then cell viability was examined by performing an MTT assay as described in MATERIALS AND METHODS. The results showed that cell viability was well maintained in CRT-underexpressing cells treated with H_2O_2 compared with the decreased viability in control and CRT-overexpressing cells. As shown in Fig. 7*C*, control, CRT-overexpressing, and CRT-underexpressing cells were exposed to 50 μM H_2O_2 for 4 h, and then the cytotoxic effect of H_2O_2 was also examined by assaying LDH release as described in MATERIALS AND METHODS. The results showed that the LDH release was suppressed more in CRT-underexpressing cells than in controls during the treatment, although the release was apparently increased in CRT-overexpressing cells. Altogether, the results show that suppression of CRT apparently enhanced cytoprotection against oxidative stress compared with controls, although overexpression of CRT increased the susceptibility to H_2O_2-induced cytotoxicity. This observation indicates that the expression level of CRT is a key factor in determining the susceptibility to H_2O_2-induced apoptosis in H9c2 cells. As shown in Fig. 7*D*, $[Ca^{2+}]_i$ was measured in control, CRT-overexpressing, and CRT-underexpressing cells after H_2O_2 treatment (75 μM) for 30 min. After the treatment with H_2O_2, the $[Ca^{2+}]_i$ increase was apparently suppressed in CRT-underexpressing cells compared with the increase in control and CRT-overexpressing cells. Collectively, the results indicate that the H_2O_2-induced $[Ca^{2+}]_i$ increase is influenced by the expression level of CRT in the cell.

Overexpression of CRT enhances processing and activation of caspase-12 through activation of calpain in H9c2 cells under oxidative stress due to H_2O_2. To further investigate the mechanism of the CRT-dependent enhancement of apoptosis through the alteration of Ca^{2+} homeostasis, we focused on caspase-12, which is activated by calpain, a Ca^{2+}-dependent cysteine protease, in ER stress-induced apoptosis (40). As shown in Fig. 8*A*, the expression levels of caspase-12 and caspase-3 and ER stress-related chaperones were examined using immunoblot analysis in control and CRT-overexpressing cells treated with 75 μM H_2O_2. In control cells, a pro-caspase form of caspase-12 (55 kDa) showed no change after 1 h of treatment with H_2O_2 but was diminished after 2 h of treatment. The level of 35-kDa proteolytic fragment of caspase-12 gradually increased during the 2-h treatment. In CRT-overexpressing cells, the level of the 55-kDa pro-caspase form was low and that of the 35-kDa fragment was rather high even under

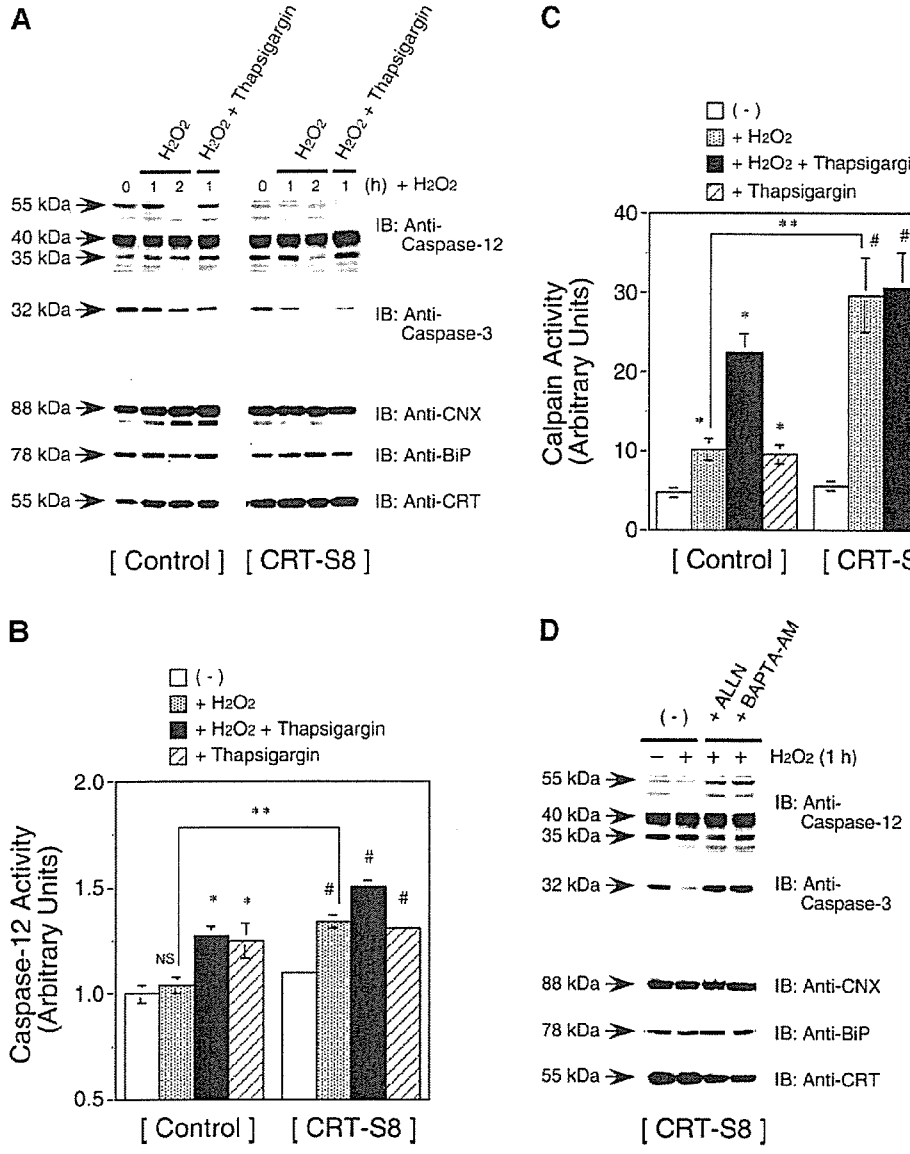

Fig. 8. The calpain-caspase-12 pathway is activated in CRT-overexpressing H9c2 cells under oxidative stress. *A*: control and CRT-overexpressing (CRT-S8) cells were exposed to 75 μM H_2O_2 for 1 and 2 h or to 75 μM H_2O_2 and 5 μM thapsigargin for 1 h, and then the expression levels of caspase-12 and caspase-3, CNX, BiP, and CRT were examined using cell lysates by performing immunoblot analysis with specific antibodies. Data represent 3 independent experiments. *B*: cells were exposed to 75 μM H_2O_2 and/or 5 μM thapsigargin for 1 h. Activity of caspase-12 was assayed with cell lysates using the substrate Ala-Thr-Ala-Asp-7-amino-4-trifluoromethylcoumarin (AFC) as described in MATERIALS AND METHODS. Each value represents the mean ± SD of 3 independent experiments. Statistical analysis was performed using a factorial ANOVA test. $^*P < 0.05$ vs. untreated control cells. $^{**}P < 0.05$ vs. control cells treated with H_2O_2. $\#P < 0.05$ vs. untreated CRT-S8 cells. NS, not significant vs. untreated control cells. *C*: cells were exposed to 75 μM H_2O_2 and/or 5 μM thapsigargin for 1 h. Activity of calpain was assayed using the calpain substrate succinyl-Leu-Leu-Val-Tyr-7-amino-4-methylcoumarin (Suc-Leu-Leu-Val-Tyr-AMC) as described in MATERIALS AND METHODS. Each value represents mean ± SD of 3 independent experiments. $^*P < 0.05$ vs. untreated control cells. $^{**}P < 0.05$ vs. control cells treated with H_2O_2. $\#P < 0.05$ vs. untreated CRT-S8 cells. *D*: CRT-overexpressing (CRT-S8) cells were treated for 1 h with or without 75 μM H_2O_2 in the presence or absence of 50 μM *N*-acetyl-leucyl-leucyl-norleucinal (ALLN) or 10 μM BAPTA-AM, and then the expression levels of caspase-12, caspase-3, CNX, BiP, and CRT were examined using cell lysates by performing immunoblot analysis with specific antibodies. Data represent 3 independent experiments.

nonstressed conditions. During treatment with H_2O_2, the 55-kDa band gradually decreased in intensity. On the other hand, the strength of the 35-kDa band was slightly increased after 1 h of treatment with H_2O_2 but was diminished after 2 h of treatment, suggesting enhanced proteolytic processing of the fragment in CRT-overexpressing cells treated with H_2O_2. The level of the 40-kDa band did not show significant change in control and CRT-overexpressing cells during treatment. These results indicate that proteolytic processing or degradation of caspase-12 was more accelerated in CRT-overexpressing cells than in control cells after treatment with H_2O_2. H_2O_2-induced processing also seemed to be enhanced by thapsigargin in both control and CRT-overexpressing cells. In the case of caspase-3, although the proteolytic cleavage was observed in control and CRT-overexpressing cells under stress due to H_2O_2, proteolysis was relatively accelerated in CRT-overexpressing cells

compared with controls. These results indicate that proteolytic processing or degradation of caspase-12 and caspase-3 is apparently accelerated in CRT-overexpressing cells under stress caused by H_2O_2. In contrast, no significant change in the expression levels of ER chaperones such as CNX, BiP, and CRT seemed to be induced by H_2O_2. Next, to investigate the relationship between proteolytic processing and the activity of caspase-12, we examined the enzyme activity of caspase-12 in cells after 1 h with or without 75 μM H_2O_2 and/or 5 μM thapsigargin (Fig. 8*B*). In CRT-overexpressing cells, activity was increased solely by H_2O_2, compared with no significant increase in activity in the control cells. Although activity was increased by thapsigargin in both control and CRT-overexpressing cells, it was elevated more in CRT-overexpressing cells during the combined treatment with H_2O_2. As shown in Fig. 8*C*, the activity of calpain was also examined in the cells after 1 h with or without 75 μM H_2O_2 and/or 5 μM thapsigargin. The activity of calpain was significantly increased by H_2O_2 in CRT-overexpressing cells compared with the small increase observed in control cells. In control cells, treatment with thapsigargin synergistically enhanced the effect of H_2O_2, although the activity was slightly increased solely by thapsigargin. In CRT-overexpressing cells, although calpain activity was markedly increased by thapsigargin, a synergistic effect was not observed. To determine whether the activity of calpain contributes to the processing of caspase-12, we examined the effect of *N*-acetyl-leucyl-leucyl-norleucinal (ALLN), a calpain inhibitor (57), or BAPTA-AM on processing in CRT-overexpressing cells during treatment with H_2O_2 (Fig. 8*D*). CRT-overexpressing cells were treated for 1 h with or without 75 μM H_2O_2 in the presence or absence of 50 μM ALLN or 10 μM BAPTA-AM, and then the expression levels of caspase-12 and caspase-3 and ER chaperones were examined using immunoblot analysis. The H_2O_2-induced processing of caspase-12 was apparently suppressed in the presence of ALLN or BAPTA-AM, resulting in a slight decrease in the level of the 35-kDa fragment and an increase in that of the 55-kDa procaspase form. Proteolytic processing of caspase-3 was also suppressed by ALLN or BAPTA-AM in gene-transfected cells treated with H_2O_2. Altogether, these results suggest that the Ca^{2+}-calpain pathway is involved in the activation of caspase-12 in CRT-overexpressing cells under oxidative stress caused by H_2O_2.

DISCUSSION

In the present study, we used myocardiac H9c2 cells that overexpressed CRT to investigate the effect of overexpression on H_2O_2-induced apoptosis in cardiac myocytes. When exposed to H_2O_2, the CRT-overexpressing cells showed increases in LDH release and DNA strand breaks, indicating that these cells were highly susceptible to apoptosis compared with control cells. Nakamura et al. (41) reported that overexpression of CRT resulted in increased sensitivity of HeLa cells to both thapsigargin- and staurosporine-induced apoptosis. These authors suggested that overexpression of CRT affected communication between the ER and the mitochondria to increase the sensitivity to apoptosis via the altered Ca^{2+} homeostasis, and their hypothesis has been supported by the study of Arnaudeau et al. (1). Pinton et al. (43) reported that the releasable $[Ca^{2+}]$ in the ER is important for ceramide-induced apoptosis and also showed that overexpression of CRT enhanced the ceramide-induced apoptosis in HeLa cells. Recently, it was also reported that CRT controls the susceptibility to apoptosis by regulating p53 functions (34). Furthermore, a necrosis-promoting effect of CRT has been reported to occur in *Caenorhabditis elegans* (53). In contrast, overexpression of CRT provided resistance to oxidant-induced cell death in renal epithelial LLC-PK1 cells treated with iodoacetamide (28), *tert*-butylhydroperoxide (29), or H_2O_2 (18). The function of CRT in the regulation of apoptosis may differ in specific cell types and is still controversial, so further investigation is required.

Ca^{2+} is one of the most versatile biological factors and regulates a variety of cellular events, such as cell development, cell proliferation, and cell death (3). The elevation of $[Ca^{2+}]_i$ has been thought to be an important signal in the mechanism of apoptosis (31). In the present study, we found that the level of $[Ca^{2+}]_i$ increased significantly in CRT-overexpressing cells treated with H_2O_2, although only a slight increase was observed in controls (Fig. 4). As shown in Fig. 6, H_2O_2-induced apoptosis was suppressed by the Ca^{2+} chelator BAPTA-AM in CRT gene-transfected cells but was promoted by thapsigargin in control cells, indicating that the increase in $[Ca^{2+}]_i$ was an important trigger for apoptosis in H9c2 cells under stress due to H_2O_2.

In previous reports, overexpression of CRT led to an increase in the intracellular store of Ca^{2+} (2, 8, 32, 54). CRT also appears to modulate store-operated Ca^{2+} influx (1, 2, 8, 32, 46, 54) and to alter Ca^{2+} transport by SERCA2b (22). In the case of H9c2 cells overexpressing CRT, the total cellular Ca^{2+} content examined on the basis of measuring equilibrium $^{45}Ca^{2+}$ uptake was ~160% of that in control cells and was found mainly within the thapsigargin-sensitive store. However, $[Ca^{2+}]_i$ levels in the resting state were not significantly different between control and CRT-overexpressing cells. On the other hand, store-operated Ca^{2+} influx was examined spectrofluorometrically using cells labeled with fura-2 AM and was suppressed in the CRT-overexpressing cells compared with controls (data not shown). These results indicate that overexpression of CRT influences intracellular Ca^{2+} homeostasis, and the effect in resting H9c2 cells seems to be similar to that in other cell types described in the literature. Recently, Scorrano et al. (48) reported that Ca^{2+} reserved in the ER was an important gateway for apoptosis via the influence on mitochondrial Ca^{2+} homeostasis. Overexpression of CRT also influences the mitochondrial Ca^{2+} homeostasis (1). Altogether, the enhanced susceptibility to H_2O_2-induced apoptosis in CRT-overexpressing H9c2 cells may also be due to the modulation of mitochondrial Ca^{2+} homeostasis by the altered responses in the ER overexpressing CRT.

Under oxidative stress, reactive oxygen and nitrogen can disrupt normal physiological pathways and cause cell death via altered Ca^{2+} homeostasis (7, 30). The $[Ca^{2+}]_i$ level is regulated by Ca^{2+} transport into and out of the ER or SR, in which Ca^{2+} can be stored, as well as by Ca^{2+} transport through the plasma membrane between the cytoplasm and the extracellular space (3). It was reported that oxidative stress causes a $[Ca^{2+}]_i$ increase in a variety of cell types (7). The initial increase in $[Ca^{2+}]_i$ results in part from a rapid release of ER Ca^{2+} through IP_3 receptors after receptor-mediated activation of PLC, and the subsequent generation of IP_3 and the sustained component results from the influx of extracellular Ca^{2+} (54). It is also

known that the uptake of Ca^{2+} from the cytoplasm to the ER/SR by SERCA can be inhibited by O_2^- and H_2O_2 in smooth muscle cells (14, 15). It seems that SERCA can be inhibited both by oxidation of its sulfhydryl residues and by a direct attack of oxidants on the ATP-binding site (7).

In the present study, the influx and efflux of $^{45}Ca^{2+}$ were examined in control and CRT-overexpressing cells with or without H_2O_2 treatment (Fig. 5, *A* and *B*). The results showed that Ca^{2+} influx was suppressed and that efflux was enhanced in the gene-transfected cells during H_2O_2 treatment, suggesting that the H_2O_2-induced increase in $[Ca^{2+}]_i$ might not be caused simply by the change of Ca^{2+} flux between the cytoplasm and extracellular space, but rather by the alteration in intracellular Ca^{2+} pools such as those in the ER and the mitochondria. To investigate the involvement of intracellular Ca^{2+} pools in the H_2O_2-induced increase in $[Ca^{2+}]_i$, we examined the effect of Ca^{2+} modulators on $[Ca^{2+}]_i$ in cells treated with H_2O_2 (Fig. 5*C*). The inhibition of mitochondrial function by FCCP did not enhance the H_2O_2-induced $[Ca^{2+}]_i$ increase in control cells, indicating that suppressed mitochondrial function was not a main cause of the enhancement of $[Ca^{2+}]_i$ observed in CRT-overexpressing cells. On the other hand, thapsigargin, an inhibitor for SERCA, apparently enhanced the H_2O_2-induced $[Ca^{2+}]_i$ increase in control cells, strongly suggesting that the Ca^{2+} store in the ER might be a cause of the $[Ca^{2+}]_i$ elevation observed in CRT-overexpressing cells. This observation also suggested that dysfunction of SERCA2a has a promoting effect on the H_2O_2-induced $[Ca^{2+}]_i$ increase in H9c2 cells. Although ER residents such as the ryanodine and IP_3 receptors may possibly be involved in raising $[Ca^{2+}]_i$ levels in response to H_2O_2, the inhibition of both did not suppress the H_2O_2-induced $[Ca^{2+}]_i$ increase in CRT-overexpressing cells. These results suggest that the H_2O_2-induced $[Ca^{2+}]_i$ increase may be due to a dysfunction of SERCA2a and not to the release of Ca^{2+} from the ER through the ryanodine or IP_3 receptors. However, it is noteworthy that the H_2O_2-induced increase of $[Ca^{2+}]_i$ was clearly suppressed by Ni^{2+}, an inhibitor of Ca^{2+} influx in gene-transfected cells. Collectively, these results indicate that the ER-stored Ca^{2+} pool plays an important role in the enhancement of the H_2O_2-induced $[Ca^{2+}]_i$ increase in CRT-overexpressing cells, although Ca^{2+} influx from the extracellular space was also an important contributor to the increase.

In a recently published report (15), we focused on the function of SERCA2a in CRT-overexpressing H9c2 cells under oxidative stress caused by H_2O_2 because SERCA is an ER/SR resident protein that is highly susceptible to peroxide stress. In that study, we found that in vitro activities of SERCA2a and $^{45}Ca^{2+}$ uptake into the ER were both suppressed by H_2O_2 in CRT-overexpressing H9c2 cells compared with controls (20). This finding indicates that the inactivation of SERCA2a was accelerated by the overexpression of CRT in the microsomes treated with H_2O_2. We also found that CRT transiently interacted with SERCA2a during H_2O_2-induced oxidative stress and that H_2O_2-induced degradation of SERCA2a was apparently enhanced in gene-transfected cells compared with controls. On the other hand, interaction between CRT and the IP_3 or ryanodine receptor was not detected in the cells under the same conditions (data not shown), suggesting that other Ca^{2+}-regulating proteins in the ER had little physical interaction with CRT under oxidative stress. These findings suggest that the increase in $[Ca^{2+}]_i$ may be due partly to the loss of Ca^{2+}-pumping activity of SERCA2a in the ER of CRT-overexpressing cells under oxidative stress.

Sustained elevation of the CRT level in the ER may be a consequence of ER stress. ER stress, also known as the unfolded protein response, is a physiological cellular response against accumulated misfolded proteins in the ER (25). However, prolonged ER stress is known to lead to apoptosis and to be linked to the pathogenesis of several disorders, including genetic diseases (e.g., type 1 diabetes mellitus), neurodegenerative diseases (e.g., Alzheimer disease, Parkinson disease), and metabolic diseases (e.g., hyperhomocysteinemia) (25). Caspase-12, which is associated with the ER, is specifically involved as a cell death effector via ER stress (40, 44). ER stress-induced activation of caspase-12 occurred through proteolytic processing by calpain via $[Ca^{2+}]_i$ elevation in the stressed cell (40). In the present study, we have shown that caspase-12 was highly activated in the CRT-overexpressing cells under oxidative stress through the activation of the Ca^{2+}-calpain pathway (Fig. 8). The results strongly suggest that a Ca^{2+}-calpain-caspase-12 pathway is involved in the mechanism of accelerated susceptibility to H_2O_2-induced apoptosis in CRT-overexpressing cells. Although Morishima et al. (37) did not clarify fully the precise activation mechanism for the caspase-12-related pathway, they reported that ER stress could trigger a specific cascade involving caspase-12, caspase-9, and caspase-3 in a cytochrome *c*-independent manner. This finding may be consistent with our findings that the H_2O_2-induced processing of both caspase-12 and caspase-3 was accelerated in CRT-overexpressing cells under stress and was suppressed in the presence of a calpain inhibitor, ALLN. Furthermore, the processing of caspase-12 and caspase-3 was suppressed by a Ca^{2+} chelator, BAPTA-AM, in the H_2O_2-treated, CRT-overexpressing cells, suggesting an activated linkage of the Ca^{2+}-calpain-caspase-12 signaling cascade in the apoptotic process of CRT-overexpressing cells under oxidative stress.

We also have shown that overexpression of CRT promotes apoptosis during cardiac differentiation in H9c2 cells (24). In that study, we showed that Akt signaling was suppressed in H9c2 cells overexpressing CRT via $[Ca^{2+}]_i$ increase. In addition, we recently reported (56) that cAMP response element-dependent transcriptional upregulation of the *PP2Ac-α* gene is involved in the inactivation of Akt, leading to the enhancement of oxidant-induced apoptosis in H9c2 cells under conditions in which $[Ca^{2+}]_i$ elevation is prolonged. With regard to the differentiation of cardiomyocytes, the importance of the intracellular generation of reactive oxygen species is implicated (47). In this respect, the altered Ca^{2+} homeostasis leading to accelerated apoptosis in CRT-overexpressing cells during differentiation may be related to a similar mechanism in cells to which reactive oxygen species are exposed. Moreover, in addition to the mechanism related to Akt signaling, the results of the present study also suggest that the Ca^{2+}-calpain-caspase-12 pathway is part of another mechanism of the differentiation-induced apoptosis of CRT-overexpressing H9c2 cells (24).

In conclusion, the results of the present study indicate that the level of CRT regulates susceptibility to oxidative stress through a change in Ca^{2+} homeostasis and a Ca^{2+}-dependent calpain-caspase-12 pathway in myocardiac H9c2 cells, suggesting a pathophysiological significance of CRT in myocardiac disorders under conditions of oxidative stress.